

Likelihood-Free Frequentist Inference: Bridging Classical Statistics and Machine Learning in Simulation and Uncertainty Quantification

Niccolò Dalmaso ^{*†}

NICCOLO.DALMASSO@GMAIL.COM

David Zhao ^{*†}

DAVIDZHAO@STAT.CMU.EDU

Rafael Izbicki [‡]

RAFAELIZBICKI@GMAIL.COM

Ann B. Lee [†]

ANNLEE@STAT.CMU.EDU

Abstract

Many areas of science make extensive use of computer simulators that implicitly encode likelihood functions of complex systems. Classical statistical methods are poorly suited for these so-called likelihood-free inference (LFI) settings, outside the asymptotic and low-dimensional regimes. Although new machine learning methods, such as normalizing flows, have revolutionized the sample efficiency and capacity of LFI methods, it remains an open question whether they produce reliable measures of uncertainty.

This paper presents a statistical framework for LFI that unifies classical statistics with modern machine learning to: (1) efficiently construct frequentist confidence sets and hypothesis tests with finite-sample guarantees of nominal coverage (type I error control) and power; (2) provide practical diagnostics for assessing empirical coverage over the entire parameter space. We refer to our framework as *likelihood-free frequentist inference* (LF2I). Any method that estimates a test statistic, like the likelihood ratio, can be plugged into our framework to create valid confidence sets and compute diagnostics, without costly Monte Carlo samples at fixed parameter settings. In this work, we specifically study the power of two test statistics (ACORE and BFF), which, respectively, maximize versus integrate an odds function over the parameter space. Our study offers multifaceted perspectives on the challenges in LF2I.

Keywords: likelihood-free inference, simulation-based inference, frequentist coverage, confidence sets, hypothesis testing

1. Introduction

Hypothesis testing and uncertainty quantification are the hallmarks of scientific inference. Methods that achieve good statistical performance (e.g., high power) often rely on being able to explicitly evaluate a likelihood function, which relates parameters of the data-generating process to observed data. However, in many areas of science and engineering, complex phenomena are modeled by forward simulators that *implicitly* define a likelihood function. For example, given input parameters θ , a stochastic model may encode the interaction of atoms or elementary particles, or the transport of radiation through the atmosphere

*. Equal Contribution

†. Department of Statistics and Data Science, Carnegie Mellon University, Pittsburgh, USA

‡. Department of Statistics, Federal University of Sao Carlos, Sao Paulo, Brazil

or through matter in the Universe, by combining deterministic dynamics with random fluctuations and measurement errors to produce synthetic data \mathbf{X} .

Simulation-based inference without an explicit likelihood is commonly referred to as *likelihood-free inference* (LFI). The most well-known approach to LFI is Approximate Bayesian Computation (ABC; see Beaumont et al. 2002; Marin et al. 2012; Sisson et al. 2018 for a review). These methods use simulations sufficiently close to the observed data D to infer the underlying parameters, or more precisely, the posterior distribution $p(\theta|D)$. Recently, the arsenal of LFI methods has been expanded with new machine learning algorithms (such as neural density estimators) that instead use the output from simulators as training data. The objective here is to learn a “surrogate model” for the likelihood or posterior. The surrogate model, rather than the simulations themselves, is then used for inference.

While the field of likelihood-free inference has undergone a revolution in terms of the complexity of problems that can be tackled (see Cranmer et al. 2020 for a recent review), the development on the statistical methodology front has fallen behind. Indeed, a question that has received little attention so far is whether one, in a high-dimensional simulator-based setting, can construct practical inferential tools with finite-sample guarantees of frequentist coverage. Frequentist procedures have undoubtedly played an important role in many fields. In high energy physics (HEP), for instance, classical statistical techniques (e.g., hypothesis testing for signal detection) have resulted in discoveries of new physics and other successful applications (Feldman and Cousins, 1998; Cranmer, 2015; Tanabashi et al., 2018; Cousins, 2018). Even though controlling type I error probabilities is important in these applications, most simulator-based methods do not have theoretical guarantees on validity or power beyond low-dimensional data settings and large-sample theory assumptions (Feldman and Cousins, 1998). Some recent LFI methods (Frate et al., 2017; Brehmer et al., 2018, 2020b) are able to compute frequentist confidence sets for high-dimensional data, but then either use the asymptotic properties of the likelihood ratio function, or rely on simulating a large number of Monte Carlo (MC) toy experiments at fixed parameter points (Brehmer et al., 2020a, Section IIB). An open question is: can we provide both scalable procedures and theoretical guarantees for constructing valid confidence sets and for performing diagnostics?

In this paper, we present a statistical framework for LFI which unifies classical statistics with modern machine learning (e.g., deep generative models, neural network classifiers, and quantile regression) to achieve the following goals:

- (i) efficiently compute confidence sets and hypothesis tests with finite-sample guarantees of frequentist coverage (nominal type I error) and power,
- (ii) estimate empirical coverage over the entire parameter space,
- (iii) present general procedures that scale with both feature and parameter dimension, and
- (iv) provide insight as to the sources of errors in LFI — both statistical errors (due to finite number of observations or simulations) and numerical errors (due to choice of optimization or integration algorithm) — which may lead to a decrease in power.

At the heart of our proposed framework is the *Neyman construction of confidence sets* (Figure 2) — a procedure that is widely known and cited, but which nevertheless has not translated to practical algorithms for high-dimensional data and complex settings beyond

asymptotic approximations. The main bottleneck has been that the construction of confidence sets requires one to consider the null hypothesis $H_{0,\theta_0} : \theta = \theta_0$ versus the alternative hypothesis $H_{0,\theta_0} : \theta \neq \theta_0$ for *every* θ_0 -value in the entire parameter space Θ since the critical value (for type I control) and the p-value will depend on θ_0 (Brehmer et al., 2020a). On a related note, scientists have long recognized the importance of checking coverage of constructed confidence sets over *all* parameters, but computationally this has been infeasible; see, e.g., Cousins 2018, Section 13 for a discussion of evaluation of coverage with toy MC simulation.

This work introduces inferential and diagnostic tools that scale with both parameter and feature dimension. Our main observation is that key quantities of interest in frequentist statistical inference — test statistics, critical values, p-values and confidence set coverage — are conditional functions of the (unknown) parameter, and generally vary smoothly over the parameter space. As a result, one can leverage machine learning methods and data simulated in the neighborhood of a parameter to improve estimates of quantities of interest with fewer total simulations. Here, we propose probabilistic classification for computing test statistics, quantile regression for estimating critical values, and regression for computing p-values and empirical coverage, as continuous functions of the parameter $\theta \in \Theta$.

Figure 1 illustrates our inference machinery. It has three main branches: First, we simulate a sample \mathcal{T} to train a probabilistic classifier for learning a parametrized “odds function” (center branch); as we shall see, this function can be used to construct meaningful test statistics (Section 3.2). We then simulate a second sample \mathcal{T}' to estimate critical values or p-values (left branch) for efficient construction of confidence sets (Section 3.3). Finally, we create a third sample \mathcal{T}'' to assess empirical coverage across the parameter space (right branch; Section 3.4). Each branch of our inference machinery is modular. Of particular note, is that (i) *any* test statistic defined in an LFI setting can be used to construct confidence sets with finite validity via the left branch, and (ii) our diagnostic procedures can provide insights to any LFI inference method via the right branch.

The ACORE (Approximate Computation via Odds Ratio Estimation; Dalmaso et al. 2020) statistic is an example of a test statistic that has good frequentist properties when combined with our modular framework. ACORE is easy to interpret: by drawing synthetic data from a simulator F_θ and comparing the data to a sample from a reference distribution G , the algorithm estimates a parametrized odds function $\mathbb{O}(\mathbf{X}; \theta)$ via probabilistic classification. When the odds function $\mathbb{O}(\mathbf{x}; \theta)$ is well-estimated for every θ and \mathbf{x} , then an estimate of the ACORE statistic (Equation 6) is the same as the well-known likelihood ratio statistic. However, in this paper, we highlight that there are LFI scenarios where one might benefit from targeting a statistic that is not the likelihood ratio statistic. Specifically, we bring attention to the Bayes factor (Jeffreys, 1935, 1961) as a frequentist test statistic in LFI. We refer to our frequentist LFI approach with estimated odds and calibrated critical values as *Bayes Frequentist Factor* inference, or BFF for short. Because BFF integrates (rather than maximizes) an estimate of $\mathbb{O}(\mathbf{X}; \theta)$ over the parameter space, it sometimes leads to statistical procedures that are more stable and powerful in practice. Robustness is especially important in high-dimensional parameter spaces and in situations where the estimated odds function has spurious spikes.

This work represents a multi-faceted study of *likelihood-free frequentist inference*, or LF2I for short. It includes both a theoretical analysis of LFI procedures, as well as an

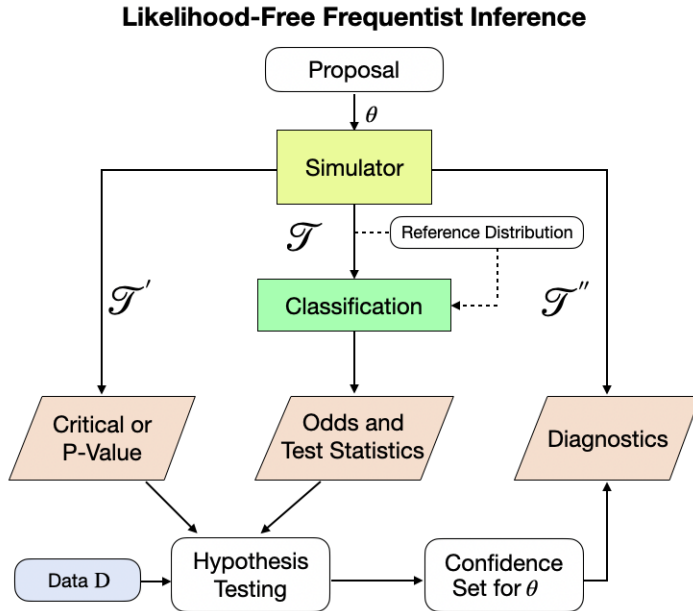


Figure 1: Schematic diagram of likelihood-free frequentist inference (LF2I). The simulator provides synthetic observable data \mathcal{T} for learning a parametrized odds function via probabilistic classification. The simulator also generates a separate sample \mathcal{T}' for learning critical values or p-values as a function of $\theta \in \Theta$. Once data D are observed, the BFF or ACORE statistics can be used to construct hypothesis tests and confidence sets for θ . Our framework also provides diagnostics for computing the empirical coverage of constructed confidence sets as a function of the (unknown) parameter θ . The three main parts of the inference machinery (critical or p-value estimation, odds estimation, diagnostics) are separate modules. Each module leverages machine learning methods in the training phase and is amortized, i.e., it performs inference on new data without having to be retrained.

attempt to understand practical considerations and performance in LF2I. In Section 4 and Appendix D, we prove that BFF and ACORE lead to valid hypothesis tests and confidence sets in the finite- n regime, as long as we have a large enough sample \mathcal{T}' to estimate critical values or p-values (Theorems 1 and 2). These results hold regardless of whether we estimate the test statistics well or not. In terms of power, BFF and ACORE converge to the power of the corresponding exact tests (the Bayes Factor and the likelihood ratio test, respectively), as long as the critical values or p-values are well estimated and the sample \mathcal{T} for estimating odds is large enough. For BFF, we can directly relate statistical power to a loss function that is easy to compute in practice (Theorem 3). Hence, we can provide convergence rates for BFF to the exact Bayes factor test for some known probabilistic classifiers (Theorem 4).

In traditional statistical inference, confidence sets are solely determined by the choice of test statistic, the assumed distribution of the test statistic under the null, and the amount of available data. In LFI, however, we note that there exist additional sources of errors that ultimately determine validity and power; we outline these sources in Section 5. In Section 6, we propose procedures for handling nuisance parameters. Section 7 demonstrates the efficacy of ACORE and BFF for some well-known synthetic examples with, for example, intractable null distribution, increasing dimension or nuisance parameters.

1.1 Relation to Other Work

Our work unifies and draws on different ideas in the statistics and machine learning (ML) literature:

Classical statistical inference. The construction of valid hypothesis tests and confidence sets has a long history in statistics (Fisher, 1925; Neyman, 1935) with the equivalence between tests and confidence sets formalized by Neyman (1937). Often, the validity of these methods relies on large sample asymptotic theory and assumptions under which the limiting null distribution of the classical likelihood ratio statistic is known (Neyman and Pearson, 1928; Wilks, 1938). Our LFI framework is founded on the Neyman construction of confidence sets, but provides statistical procedures and theoretical guarantees for the finite-sample regime and settings with intractable limiting distributions. Furthermore, unlike more recent Monte Carlo approaches (Weinzierl, 2000; Schafer and Stark, 2009), our approach is amortized and does not require multiple MC samples at each parameter value θ for constructing confidence sets.

Universal inference. Recently, Wasserman et al. (2020) proposed a “universal” inference test statistic for constructing valid confidence sets and hypothesis tests with finite-sample guarantees without regularity conditions. The assumptions are that the likelihood $\mathcal{L}(\mathcal{D}; \theta)$ is known and that one can compute the maximum likelihood estimator (MLE). Our LFI framework does not require a tractable likelihood, but on the other hand our procedures implicitly assume that key quantities of interest vary smoothly in θ . Another main difference is that our approach estimates the critical value as a function of θ . The latter calibration step leads to more powerful tests than universal inference (see, for example, Section 7.2.1) but at the cost of having to simulate data from the likelihood.

Likelihood-free inference via machine learning. Recent LFI methods have been using the output from simulators as training data to learn a surrogate model for inference; see Cranmer et al. (2020) for a review. These LFI methods use synthetic data simulated across the parameter space to directly estimate key quantities, such as:

1. *posteriors* $p(\theta|\mathbf{x})$ (Marin et al., 2016; Papamakarios and Murray, 2016; Lueckmann et al., 2017; Greenberg et al., 2019; Chen and Gutmann, 2019; Izbicki et al., 2019; Radev et al., 2020),
2. *likelihoods* $p(\mathbf{x}|\theta)$ (Wood, 2010; Meeds and Welling, 2014; Wilkinson, 2014; Gutmann and Corander, 2016; Fasiolo et al., 2018; Lueckmann et al., 2019; Papamakarios et al., 2019; Picchini et al., 2020; Järvenpää et al., 2021), or
3. *density ratios*, such as the likelihood-to-marginal ratio $p(\mathbf{x}|\theta)/p(\mathbf{x})$ (Izbicki et al., 2014; Thomas et al., 2021; Hermans et al., 2020; Durkan et al., 2020), or the likelihood ratio $p(\mathbf{x}|\theta_1)/p(\mathbf{x}|\theta_2)$ for $\theta_1, \theta_2 \in \Theta$ (Cranmer et al., 2015; Brehmer et al., 2020b).¹

1. **ACORE** and **BFF** are based on estimating the odds $\mathbb{O}(\mathbf{X}; \theta)$ at $\theta \in \Theta$ (Equation 5); this is a “likelihood-to-marginal ratio” approach, which estimates a one-parameter function as in the original paper by Izbicki et al. (2014). The likelihood ratio $\mathbb{O}\mathbb{R}(\mathbf{X}; \theta_0, \theta_1)$ at $\theta_0, \theta_1 \in \Theta$ (Equation 7) is then computed from the odds function, without the need for an extra estimation step.

Undoubtedly, new ML methods, such as normalizing flows (Papamakarios et al., 2021) and other neural density estimators, have revolutionized and will continue to revolutionize the development in LFI in terms of sample efficiency and capacity. However, although the goal of LFI is inference on the unknown parameters θ , it remains an open question whether a given LFI algorithm produces reliable measures of uncertainty. A related question is how to objectively evaluate the power and coverage of various approaches when the true θ of interest is not known.

Our framework can lend good statistical properties and theoretical guarantees of nominal coverage to any LFI algorithm that computes a “test statistic”; that is, a measure of how well observed data fits the conjecture that the true parameter θ has a certain value θ_0 . Furthermore, we provide diagnostic tools that assess whether constructed confidence sets and tests are valid for any value in the parameter space. To the best of our knowledge, no other LFI methodology can guarantee statistical validity and power in a finite-sample regime (without costly Monte Carlo samples at fixed parameter values), as well as provide practical diagnostics for assessing coverage across the entire parameter space (when the true solution is not known).

Notation. Let F_θ with density f_θ represent the stochastic forward simulator for a sample point $\mathbf{X} \in \mathcal{X}$ at parameter $\theta \in \Theta$. We denote i.i.d “observable” data from F_θ by $\mathcal{D} = \{\mathbf{X}_1^{\text{obs}}, \dots, \mathbf{X}_n^{\text{obs}}\}$, and the actually observed or measured data by $D = \{\mathbf{x}_1^{\text{obs}}, \dots, \mathbf{x}_n^{\text{obs}}\}$. The likelihood function $\mathcal{L}(\mathcal{D}; \theta) = \prod_{i=1}^n f_\theta(\mathbf{X}_i^{\text{obs}})$.

2. Statistical Inference in a Traditional Setting

We begin by reviewing elements of traditional statistical inference that play a key role in our framework for likelihood-free frequentist inference.

Equivalence of Tests and Confidence Sets. A classical approach to constructing a confidence set for an unknown parameter $\theta \in \Theta$ is to invert a series of hypothesis tests (Neyman, 1937): Suppose that for each possible value $\theta_0 \in \Theta$, there is a level α test δ_{θ_0} of

$$H_{0,\theta_0} : \theta = \theta_0 \quad \text{versus} \quad H_{1,\theta_0} : \theta \neq \theta_0; \quad (1)$$

that is, a test δ_{θ_0} where the type I error (the probability of erroneously rejecting a true null hypothesis H_{0,θ_0}) is no larger than α . For observed data $\mathcal{D} = D$, now define $R(D)$ as the set of all parameter values $\theta_0 \in \Theta$ for which the test δ_{θ_0} does not reject H_{0,θ_0} . Then, by construction, the random set $R(\mathcal{D})$ satisfies

$$\mathbb{P}[\theta_0 \in R(\mathcal{D}) \mid \theta = \theta_0] \geq 1 - \alpha$$

for all $\theta_0 \in \Theta$. That is, $R(\mathcal{D})$ defines a $(1 - \alpha)$ *confidence set* for θ . Similarly, we can define tests with a desired significance level by inverting a confidence set with a certain coverage.

Likelihood Ratio Test. A general form of hypothesis tests that often leads to high power is the likelihood ratio test (LRT). Consider testing

$$H_0 : \theta \in \Theta_0 \quad \text{versus} \quad H_1 : \theta \in \Theta_1, \quad (2)$$

where $\Theta_1 = \Theta \setminus \Theta_0$. For the *likelihood ratio (LR) statistic*,

$$\text{LR}(\mathcal{D}; \Theta_0) = \log \frac{\sup_{\theta \in \Theta_0} \mathcal{L}(\mathcal{D}; \theta)}{\sup_{\theta \in \Theta} \mathcal{L}(\mathcal{D}; \theta)}, \quad (3)$$

the LRT of hypotheses (2) rejects H_0 when $\text{LR}(\mathcal{D}; \Theta_0) < C$ for some constant C .

Figure 2 illustrates the construction of confidence sets for θ from level α likelihood ratio tests (1). The critical value for each such test δ_{θ_0} is $C_{\theta_0} = \sup \{C : \mathbb{P}(\text{LR}(\mathcal{D}; \theta_0) < C \mid \theta = \theta_0) \leq \alpha\}$.

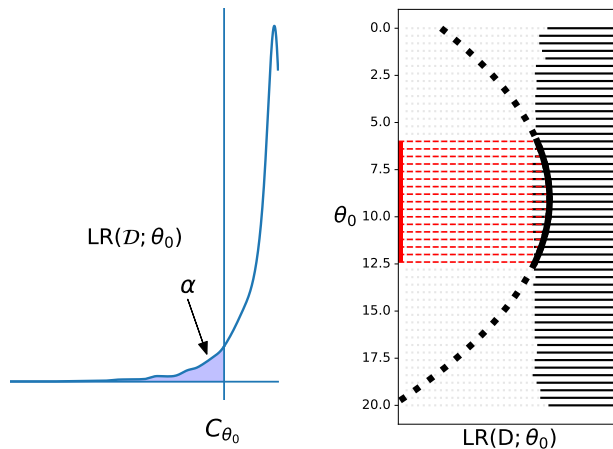


Figure 2: Constructing confidence intervals from hypothesis tests. *Left*: For each $\theta_0 \in \Theta$, we find the critical value C_{θ_0} that rejects the null hypothesis H_{0,θ_0} at level α ; that is, C_{θ_0} is the α -quantile of the distribution of the likelihood ratio statistic $\text{LR}(\mathcal{D}; \theta_0)$ under the null. *Right*: The horizontal lines represent the acceptance region for each $\theta_0 \in \Theta$. Suppose we observe data $\mathcal{D} = D$. The confidence set for θ (indicated with the red line) consists of all θ_0 -values for which the observed test statistic $\text{LR}(D; \theta_0)$ (indicated with the black curve) falls in the acceptance region.

Bayes Factor. Let π be a probability measure over the parameter space Θ . The Bayes factor (Jeffreys, 1935, 1961) for comparing the hypothesis $H_0 : \theta \in \Theta_0$ to its complement, the alternative H_1 , is a ratio of the marginal likelihood of the two hypotheses:

$$\text{BF}(\mathcal{D}; \Theta_0) \equiv \frac{\mathbb{P}(\mathcal{D}|H_0)}{\mathbb{P}(\mathcal{D}|H_1)} = \frac{\int_{\Theta_0} \mathcal{L}(\mathcal{D}; \theta) d\pi_0(\theta)}{\int_{\Theta_1} \mathcal{L}(\mathcal{D}; \theta) d\pi_1(\theta)}, \quad (4)$$

where π_0 and π_1 are the restrictions of π to the parameter regions Θ_0 and $\Theta_1 = \Theta_0^c$, respectively. The Bayes factor is often used as a Bayesian alternative to significance testing, as it quantifies the change in the odds in favor of H_0 when going from the prior to the posterior: $\frac{\mathbb{P}(H_0|\mathcal{D})}{\mathbb{P}(H_1|\mathcal{D})} = \text{BF}(\mathcal{D}; \Theta_0) \frac{\mathbb{P}(H_0)}{\mathbb{P}(H_1)}$.

3. Likelihood-Free Frequentist Inference

In the typical LFI setting, we cannot directly evaluate the likelihood ratio $\text{LR}(\mathcal{D}; \Theta_0)$, or even the likelihood $\mathcal{L}(\mathcal{D}; \theta)$. A simulator-based approach with, for example, **ACORE** or **BFF** can nevertheless lead to hypothesis tests and confidence sets with good frequentist properties. The assumptions are access to: (i) a “high-fidelity” forward simulator, also denoted by F_θ , that can simulate observable data, (ii) a reference distribution G , which does not depend on θ , with larger support than F_θ for all $\theta \in \Theta$, and (iii) a probabilistic classifier that discriminates samples from F_θ and G .

3.1 Parametrized Odds for Labeled Samples

We start by generating a labeled sample $\mathcal{T} = \{\theta_i, \mathbf{X}_i, Y_i\}_{i=1}^B$ to compare data from the simulator F_θ with data from the reference distribution G . Here, $\theta \sim \pi_\Theta$ (a fixed proposal distribution over Θ), the “label” $Y \sim \text{Ber}(p)$, $\mathbf{X}|\theta, Y = 1 \sim F_\theta$, and $\mathbf{X}|\theta, Y = 0 \sim G$. We then define the odds at θ and fixed \mathbf{X} as

$$\mathbb{O}(\mathbf{X}; \theta) := \frac{\mathbb{P}(Y = 1 | \theta, \mathbf{X})}{\mathbb{P}(Y = 0 | \theta, \mathbf{X})}. \quad (5)$$

One way of interpreting the odds $\mathbb{O}(\mathbf{X}; \theta)$ is to regard it as a measure of the chance that \mathbf{X} was generated from F_θ rather than from G . That is, a large odds $\mathbb{O}(\mathbf{X}; \theta)$ reflects the fact that it is plausible that \mathbf{X} was generated from F_θ (instead of G). We call G a “reference distribution” as we are comparing F_θ for different θ with this distribution.

The odds function $\mathbb{O}(\mathbf{X}; \theta)$ with $\theta \in \Theta$ as a parameter can be learned with a probabilistic classifier, such as a neural network with a softmax layer, suitable for the data \mathbf{X} at hand. Algorithm 3 in Appendix A summarizes our procedure for simulating a labeled sample \mathcal{T} for estimating odds. For all experiments in this paper, we use $p=1/2$ and $G = F_{\mathbf{X}}$, where $F_{\mathbf{X}}$ is the marginal distribution of F_θ with respect to π_Θ .

3.2 Test Statistics Based on Odds

For testing $H_{0, \Theta_0} : \theta \in \Theta_0$ versus all alternatives $H_{1, \Theta_0} : \theta \notin \Theta_0$, we consider two test statistics: **ACORE** and **BFF**. Both statistics are based on $\mathbb{O}(\mathbf{X}; \theta)$, but whereas **ACORE** eliminates the parameter θ by maximization, **BFF** averages over the parameter space.

3.2.1 ACORE BY MAXIMIZATION

The **ACORE** statistic (Dalmaso et al., 2020) for testing (1) is given by

$$\begin{aligned} \Lambda(\mathcal{D}; \Theta_0) &:= \log \frac{\sup_{\theta_0 \in \Theta_0} \prod_{i=1}^n \mathbb{O}(\mathbf{X}_i^{\text{obs}}; \theta_0)}{\sup_{\theta \in \Theta} \prod_{i=1}^n \mathbb{O}(\mathbf{X}_i^{\text{obs}}; \theta)} \\ &= \sup_{\theta_0 \in \Theta_0} \inf_{\theta_1 \in \Theta} \sum_{i=1}^n \log \left(\mathbb{O}\mathbb{R}(\mathbf{X}_i^{\text{obs}}; \theta_0, \theta_1) \right), \end{aligned} \quad (6)$$

where the odds ratio

$$\mathbb{O}\mathbb{R}(\mathbf{X}; \theta_0, \theta_1) := \frac{\mathbb{O}(\mathbf{X}; \theta_0)}{\mathbb{O}(\mathbf{X}; \theta_1)} \quad (7)$$

at $\theta_0, \theta_1 \in \Theta$ measures the plausibility that \mathbf{X} was generated from θ_0 rather than θ_1 .

We use $\widehat{\Lambda}(\mathcal{D}; \Theta_0)$ to denote the **ACORE** statistic based on \mathcal{T} and estimated odds $\widehat{\mathbb{O}}(\mathbf{X}; \theta_0)$. When $\widehat{\mathbb{O}}(\mathbf{X}; \theta_0)$ is well-estimated for every θ and \mathbf{X} , the estimated **ACORE** statistic $\widehat{\Lambda}(\mathcal{D}; \Theta_0)$ is the same as the likelihood ratio statistic $\text{LR}(\mathcal{D}; \Theta_0)$ (Dalmasso et al. 2020; Proposition 3.1).

3.2.2 BFF BY AVERAGING

Because the **ACORE** statistics in Equation 6 involves taking the supremum (or infimum) over Θ , it may not be practical in high dimensions. Hence, in this work, we propose an alternative statistic for testing (1) based on averaged odds:

$$\tau(\mathcal{D}; \Theta_0) := \frac{\int_{\Theta_0} \prod_{i=1}^n \mathbb{O}(\mathbf{X}_i^{\text{obs}}; \theta) d\pi_0(\theta)}{\int_{\Theta_0^c} \prod_{i=1}^n \mathbb{O}(\mathbf{X}_i^{\text{obs}}; \theta) d\pi_1(\theta)}, \quad (8)$$

where π_0 and π_1 are the restrictions of the proposal distribution π to the parameter regions Θ_0 and Θ_0^c , respectively.

Let $\widehat{\tau}(\mathcal{D}; \Theta_0)$ denote estimates based on \mathcal{T} and $\widehat{\mathbb{O}}(\theta_0; \mathbf{x})$. If the probabilities learned by the classifier are well estimated, then the estimated averaged odds statistic $\widehat{\tau}(\mathcal{D}; \Theta_0)$ is exactly the Bayes factor:

Proposition 1 (Fisher consistency)

If $\widehat{\mathbb{P}}(Y = 1|\theta, \mathbf{x}) = \mathbb{P}(Y = 1|\theta, \mathbf{x})$ for every θ and \mathbf{x} , then $\widehat{\tau}(\mathcal{D}; \Theta_0)$ is the Bayes factor $BF(\mathcal{D}; \Theta_0)$.

In this paper, we are using the Bayes factor as a frequentist test statistic. Hence, our term *Bayes Frequentist Factor (BFF)* statistic for τ and $\widehat{\tau}$.

3.3 Efficient Construction of Finite-Sample Confidence Sets

Although the Neyman construction of confidence sets (Figure 2) is widely known, this procedure has not translated to practical machine learning algorithms for complex data settings. Here, we address the question: How do we *efficiently* estimate critical values and significance probabilities (p-values) of a test when we do not know the distribution of our test statistic, and cannot rely on large-sample theory approximations?

Simulation-based approaches are often used to compute rejection probabilities and critical values in lieu of large-sample theory approximations. Typically, such simulations compute a separate Monte Carlo simulation at each fixed $\theta_0 \in \Theta$ on, e.g., a fine enough grid in parameter space. That is, the convention is to rely solely on sample points generated at fixed θ_0 to estimate the rejection probabilities. What we do instead is to treat the critical value C or the p -value as functions that vary smoothly with the parameter θ ; we then estimate the parametrized functions C_{θ_0} and $p(\mathcal{D}; \theta_0)$ for any $\theta_0 \in \Theta$ via quantile regression (Section 3.3.1) and regression (Section 3.3.2), respectively.

3.3.1 THE CRITICAL VALUE VIA QUANTILE REGRESSION

Rather than repeatedly running a separate procedure for each null hypothesis $H_{0, \theta_0} : \theta = \theta_0$, we use quantile regression (e.g., Meinshausen 2006; Koenker et al. 2017) to estimate the

critical values C_{θ_0} at level α for all $\theta_0 \in \Theta$ simultaneously; see Algorithm 1. This procedure is the same for BFF as for ACORE (Dalmaso et al., 2020); in fact, it is applicable to *any* test statistic λ , even beyond the LFI setting.

To test a composite null hypothesis $H_0 : \theta \in \Theta_0$ versus $H_1 : \theta \in \Theta_1$, we use the cutoff $\widehat{C}_{\Theta_0} := \inf_{\theta \in \Theta_0} \widehat{C}_\theta$. This cutoff leads to a valid test (control of type I error as the number of simulations $B' \rightarrow \infty$) for the test statistic λ , regardless of the data sample size n and choice of λ (Theorem 5, Appendix D). In particular, the calibration controls type I error for BFF and ACORE, even if the estimated statistics are not good approximations of the Bayes Factor and the LR statistic, respectively.

Algorithm 1 Estimate the critical values C_{θ_0} for a level- α test of $H_{0,\theta_0} : \theta = \theta_0$ vs. $H_{1,\theta_0} : \theta \neq \theta_0$ for all $\theta_0 \in \Theta$ simultaneously

Require: stochastic forward simulator F_θ ; sample size B' for training quantile regression estimator; π (a fixed proposal distribution over the parameter space Θ); test statistic λ ; quantile regression estimator; desired level $\alpha \in (0, 1)$

Ensure: estimated critical values \widehat{C}_{θ_0} for all $\theta_0 \in \Theta$

- 1: Set $\mathcal{T}' \leftarrow \emptyset$
 - 2: **for** i in $\{1, \dots, B'\}$ **do**
 - 3: Draw parameter $\theta_i \sim \pi_\Theta$
 - 4: Draw sample $\mathbf{X}_{i,1}, \dots, \mathbf{X}_{i,n} \stackrel{iid}{\sim} F_{\theta_i}$
 - 5: Compute test statistic $\lambda_i \leftarrow \lambda((\mathbf{X}_{i,1}, \dots, \mathbf{X}_{i,n}); \theta_i)$
 - 6: $\mathcal{T}' \leftarrow \mathcal{T}' \cup \{(\theta_i, \lambda_i)\}$
 - 7: **end for**
 - 8: Use \mathcal{T}' to learn parametrized function $\widehat{C}_\theta := \widehat{F}_{\lambda|\theta}^{-1}(\alpha|\theta)$ via quantile regression of λ on θ
 - 9: **return** \widehat{C}_{θ_0}
-

3.3.2 THE P-VALUE VIA REGRESSION

If the data D are observed beforehand, then given any test statistic λ , we can alternatively compute p-values for each hypothesis $H_{0,\theta_0} : \theta = \theta_0$, that is,

$$p(D; \theta_0) := \mathbb{P}_{\mathcal{D}|\theta_0}(\lambda(\mathcal{D}; \theta_0) < \lambda(D; \theta_0)).$$

The p-value $p(D; \theta_0)$ can be used to test hypothesis and create confidence sets for any desired level α . We can estimate these p-values by noticing that they are defined by a regression $\mathbb{E}[Z|\theta_0]$ of the random variable $Z := \mathbb{I}(\lambda(\mathcal{D}; \theta_0) < \lambda(D; \theta_0))$ on θ_0 . Thus, we can as in Algorithm 2 generate a training sample $\mathcal{T}' = \{(Z_1, \theta_1), \dots, (Z_{B'}, \theta_{B'})\}$ and then estimate p-values for all $\theta_0 \in \Theta$ simultaneously. An advantage of using a regression instead of a quantile regression approach (as in Section 3.3.1) is that we can take advantage of the many existing regression methods.

For testing the composite null hypothesis $H_0 : \theta \in \Theta_0$ versus $H_1 : \theta \in \Theta_1$, we use

$$\widehat{p}(D; \Theta_0) := \sup_{\theta \in \Theta_0} \widehat{p}(D; \theta)$$

with

$$\widehat{p}(D; \theta) := \widehat{\mathbb{P}}_{\mathcal{D}|\theta_0}(\lambda(\mathcal{D}; \theta_0) < \lambda(D; \theta_0)). \quad (9)$$

Algorithm 2 Estimate the p-values $p(D; \theta_0)$, given observed data D , for a level- α test of $H_{0, \theta_0} : \theta = \theta_0$ vs. $H_{1, \theta_0} : \theta \neq \theta_0$ for all $\theta_0 \in \Theta$ simultaneously.

Require: observed data D ; stochastic forward simulator F_θ ; sample size B' for p-value estimation; π_Θ (a fixed proposal distribution over the parameter space Θ); test statistic λ ; regression estimator m

Ensure: estimated p-value $\hat{p}(D; \theta)$ for all $\theta = \theta_0 \in \Theta$

- 1: Set $\mathcal{T}' \leftarrow \emptyset$
 - 2: **for** i in $\{1, \dots, B'\}$ **do**
 - 3: Draw parameter $\theta_i \sim \pi_\Theta$
 - 4: Draw sample $\mathbf{X}_{i,1}, \dots, \mathbf{X}_{i,n} \stackrel{iid}{\sim} F_{\theta_i}$
 - 5: Compute test statistic $\lambda_i \leftarrow \lambda((\mathbf{X}_{i,1}, \dots, \mathbf{X}_{i,n}); \theta_i)$
 - 6: Compute indicator $Z_i \leftarrow \mathbb{I}(\lambda_i < \lambda(D; \theta_i))$
 - 7: $\mathcal{T}' \leftarrow \mathcal{T}' \cup \{(\theta_i, Z_i)\}$
 - 8: **end for**
 - 9: Use \mathcal{T}' to learn parametrized function $\hat{p}(D; \theta) := \widehat{\mathbb{E}}[Z|\theta]$ via regression of Z on θ using regression estimator m
 - 10: **return** $\hat{p}(D; \theta_0)$
-

3.4 Confidence Sets and Diagnostics

Finally, we construct an approximate confidence region for θ by taking the set

$$\widehat{R}(D) = \left\{ \theta_0 \in \Theta \mid \lambda(D; \theta_0) \geq \widehat{C}_{\theta_0} \right\}, \quad (10)$$

or alternatively,

$$\widehat{R}(D) = \{ \theta_0 \in \Theta \mid \hat{p}(D; \theta_0) > \alpha \}.$$

As shown in Dalmaso et al. (2020, Theorem 3.3), the random set $\widehat{R}(D)$ has nominal $1 - \alpha$ coverage as $B' \rightarrow \infty$ regardless of the data sample size n .

When B' is finite, our LFI framework has a separate module (“Diagnostics” in Figure 1) for evaluating “local” goodness-of-fit in different regions of the parameter space Θ . This third module estimates empirical coverage, $\mathbb{P}_{D|\theta}(\theta \in \widehat{R}(D))$, as a continuous function of $\theta \in \Theta$ using probabilistic classification and a training sample $\mathcal{T}'' = \{(\theta'_1, D'_1), \dots, (\theta'_{B''}, D'_{B''})\}$, where $\theta'_i \sim \pi_\Theta$ and $D'_i := (\mathbf{X}_{i,1}, \dots, \mathbf{X}_{i,n}) \stackrel{iid}{\sim} F_{\theta'_i}$. Our test of conditional coverage, first proposed in Dalmaso et al. (2020) with the details outlined here in Algorithm 5 of Appendix B, is able to locate regions in parameter space where estimated confidence sets might under- or over-cover. More specifically, we can assess coverage locally at any $\theta \in \Theta$, unlike standard goodness-of-fit techniques for conditional densities (Cook et al., 2006; Bordoloi et al., 2010; Talts et al., 2018; Schmidt et al., 2020), which only check for marginal coverage over Θ .

3.5 Loss Function

In this work, we use the cross-entropy loss to train probabilistic classifiers. Consider a sample point $\{\theta, \mathbf{x}, y\}$ generated according to Algorithm 3. Let p be a $\text{Ber}(y)$ distribution,

and q be a $\text{Ber}\left(\widehat{\mathbb{P}}(Y = 1|\theta, \mathbf{x})\right) = \text{Ber}\left(\frac{\widehat{\mathbb{O}}(\mathbf{x};\theta)}{1+\widehat{\mathbb{O}}(\mathbf{x};\theta)}\right)$ distribution. The *cross-entropy* between p and q is given by

$$\begin{aligned}\mathcal{L}_{\text{CE}}(\widehat{\mathbb{O}}; \{\theta, \mathbf{x}, y\}) &= -y \log\left(\frac{\widehat{\mathbb{O}}(\mathbf{x};\theta)}{1+\widehat{\mathbb{O}}(\mathbf{x};\theta)}\right) - (1-y) \log\left(\frac{1}{1+\widehat{\mathbb{O}}(\mathbf{x};\theta)}\right) \\ &= -y \log\left(\widehat{\mathbb{O}}(\mathbf{x};\theta)\right) + \log\left(1+\widehat{\mathbb{O}}(\mathbf{x};\theta)\right).\end{aligned}\tag{11}$$

For every \mathbf{x} and θ , the expected cross-entropy $\mathbb{E}[L_{\text{CE}}(\widehat{\mathbb{O}}; \{\theta, \mathbf{x}, y\})]$ is minimized by $\widehat{\mathbb{O}}(\mathbf{x};\theta) = \mathbb{O}(\mathbf{x};\theta)$. If the probabilistic classifier attains the minimum of the cross-entropy loss, then as shown in Dalmaso et al. 2020, the estimated **ACORE** statistic $\widehat{\Lambda}(\mathcal{D}; \Theta_0)$ will be equal to the likelihood ratio statistic in Equation 3. Similarly, as stated in Proposition 1, at the minimum, the estimated **BFF** statistic $\widehat{\tau}(\mathcal{D}; \Theta_0)$ is equal to the Bayes factor in Equation 4.

In the special case where G is the marginal distribution of $F_\theta(\mathbf{x})$ with respect to π , and when in addition \mathbf{x} contains all observations (that is, $\mathbf{X} = \mathcal{D}$), the denominator of the **BFF** statistic in Equation 8 is equal to one, as shown in Equation 13. The **BFF** test statistic then simply becomes the integrated odds. Hence, in addition to the standard cross-entropy loss (Equation 11), we propose an *integrated odds loss* function which is directly related to the **BFF** (integrated odds) statistic:

$$\mathcal{L}(\widehat{\mathbb{O}}, \mathbb{O}) := \int \left(\widehat{\mathbb{O}}(\mathbf{x};\theta) - \mathbb{O}(\mathbf{x};\theta)\right)^2 dG(\mathbf{x})d\pi(\theta).\tag{12}$$

In Section 4, Theorem 3, we show that the power of the **BFF** test statistic is bounded by the integrated odds loss.

4. Theoretical Guarantees

Next, we prove consistency of the p-value estimation method (Algorithm 2) and provide theoretical guarantees for the power of **BFF**. We refer the reader to Appendix D for a proof that Algorithm 1 leads to valid hypothesis tests as long as B' is large enough (Theorem 5), and that the power of the **ACORE** test converges to the power of the **LRT** as B grows (Theorem 6).

4.1 P-Value Estimation

We start by showing that the p-value estimation method described in Section 3.3.2 is consistent. The results shown here apply to any test statistic λ . That is, these results are not restricted to **BFF**.

We assume consistency in the sup norm of the regression method used to estimate the p-values:

Assumption 1 (Uniform consistency) *The regression estimator used in Equation 9 is such that*

$$\sup_{\theta} |\widehat{\mathbb{E}}_{B'}[Z|\theta] - \mathbb{E}[Z|\theta]| \xrightarrow[B' \rightarrow \infty]{a.s.} 0.$$

Examples of estimators that satisfy Assumption 1 include Bierens (1983); Hardle et al. (1984); Liero (1989); Girard et al. (2014).

The next theorem shows that the p-values obtained according to Algorithm 2 converge to the true p-values. Moreover, the power of the tests obtained using the estimated p-values converges to the power one would obtain if the true p-values could be computed.

Theorem 1 *Under Assumption 1, for every $\theta \in \Theta$,*

$$\widehat{p}(D; \Theta_0) \xrightarrow[B' \rightarrow \infty]{a.s.} p(D; \Theta_0)$$

and

$$\mathbb{P}_{\mathcal{D}, \mathcal{T}'|\theta}(\widehat{p}(D; \Theta_0) \leq \alpha) \xrightarrow{B' \rightarrow \infty} \mathbb{P}_{\mathcal{D}|\theta}(p(D; \Theta_0) \leq \alpha).$$

The next corollary shows that as $B' \rightarrow \infty$, the tests obtained using the p-values from Algorithm 2 have size α .

Corollary 1 *Under Assumption 1 and if F_θ is continuous for every $\theta \in \Theta$, then*

$$\sup_{\theta \in \Theta_0} \mathbb{P}_{\mathcal{D}, \mathcal{T}'|\theta}(\widehat{p}(D; \Theta_0) \leq \alpha) \xrightarrow{B' \rightarrow \infty} \alpha.$$

Under stronger assumptions about the regression method, it is also possible to derive rates of convergence for the estimated p-values.

Assumption 2 (Convergence rate of the regression estimator) *The regression estimator is such that*

$$\sup_{\theta} |\widehat{\mathbb{E}}[Z|\theta] - \mathbb{E}[Z|\theta]| = O_P\left(\left(\frac{1}{B'}\right)^r\right).$$

for some $r > 0$.

Examples of regression estimators that satisfy Assumption 2 can be found in Stone (1982); Hardle et al. (1984); Donoho (1994); Yang et al. (2017).

Theorem 2 *Under Assumption 2,*

$$|p(D; \Theta_0) - \widehat{p}(D; \Theta_0)| = O_P\left(\left(\frac{1}{B'}\right)^r\right).$$

4.2 Power of BFF

In this section, we provide convergence rates for BFF and show that its power relates to the loss function of Equation 12.

We assume that $G(\mathbf{x})$ is the marginal distribution of $F_\theta(\mathbf{x})$ with respect to $\pi(\theta)$. We here also assume that \mathbf{x} contains all observations; that is, $\mathbf{X} = \mathcal{D}$. In this case, the denominator of the average odds is

$$\int_{\Theta} \mathbb{O}(\mathbf{x}, \theta) d\pi(\theta) = \int_{\Theta_1} \frac{f(\mathbf{x}|\theta)}{g(\mathbf{x})} d\pi(\theta) = \int_{\Theta} \frac{f(\mathbf{x}|\theta)}{\int_{\Theta} f(\mathbf{x}|\theta) d\pi(\theta)} d\pi(\theta) = 1, \quad (13)$$

and therefore there is no need to estimate the denominator in Equation 8.

We also make the following assumptions:

Assumption 3 (Bounded odds and estimated odds) *There exists $0 < M, m < \infty$ such that for every $\theta \in \Theta$ and $\mathbf{x} \in \mathcal{X}$, $m \leq \mathbb{O}(\mathbf{x}; \theta), \widehat{\mathbb{O}}(\mathbf{x}; \theta) \leq M$.*

Assumption 4 (Bounded second moment of odds estimation error) *Let*

$$h(\theta) = \int (\mathbb{O}(\mathbf{x}; \theta) - \widehat{\mathbb{O}}(\mathbf{x}; \theta))^2 dG(\mathbf{x}).$$

There exists $M', m' > 0$ such that $h(\theta) \leq M'$ and $\int h(\theta) d\pi(\theta) > m'$.

Assumption 3 states that the odds and estimated odds are both bounded away from 0 and infinity, for all choice of parameters θ and features \mathbf{x} . Assumption 4 states that the second moment of the difference between the true and estimated odds is bounded away from 0 and infinity.

Finally, we assume that the CDF of the power function of the test based on the BFF statistic τ in Equation 8 is smooth in a Lipschitz sense:

Assumption 5 (Smooth power function) *The cumulative distribution function of $\tau(\mathcal{D}; \theta_0)$, F_τ , is Lipschitz with constant C_L , i.e., for every $x_1, x_2 \in \mathbb{R}$, $|F_\tau(x_1) - F_\tau(x_2)| \leq C_L|x_1 - x_2|$.*

With these assumptions, we can relate the odds loss with the probability that the outcome of BFF is different from the outcome of the test based on the Bayes factor:

Theorem 3 *Let $\phi_\tau(\mathcal{D}) = \mathbb{I}(\tau(\mathcal{D}; \theta_0) < c)$ and $\phi_{\widehat{\tau}_B}(\mathcal{D}) = \mathbb{I}(\widehat{\tau}_B(\mathcal{D}; \theta_0) < c)$ be the testing procedures for testing $H_{0, \theta_0} : \theta = \theta_0$ obtained using τ and $\widehat{\tau}_B$. Under Assumptions 3-5, there exists $K' > 0$ such that, for every $0 < \epsilon < 1$,*

$$\mathbb{P}_{\mathcal{D}|\theta, T}(\phi_\tau(\mathcal{D}) \neq \phi_{\widehat{\tau}_B}(\mathcal{D})) \leq \frac{K' \cdot \sqrt{L(\widehat{\mathbb{O}}, \mathbb{O})}}{\epsilon} + \epsilon,$$

where T denotes the observed training sample \mathcal{T} .

Theorem 3 demonstrates that the probability that hypothesis tests based on the BFF statistic versus the Bayes factor lead to different conclusions is bounded by the integrated odds loss. This result is valuable because the integrated odds loss is easy to estimate in practice, and hence provides us with a practically useful metric. For instance, the integrated odds loss can serve as a natural criterion for selecting the “best” statistical model out of a set of candidate models with different classifiers, for tuning model hyperparameters, and for evaluating model fit.

Next, we provide rates of convergence of the test based on BFF to the test based on the Bayes factor. We assume that the chosen probabilistic classifier has the following rate of convergence:

Assumption 6 (Convergence rate of the probabilistic classifier) *The probabilistic classifier trained with \mathcal{T} , $\widehat{\mathbb{P}}(Y = 1|\mathbf{x}, \theta)$ is such that*

$$\mathbb{E}_{\mathcal{T}} \left[\int \left(\widehat{\mathbb{P}}(Y = 1|\mathbf{x}, \theta) - \mathbb{P}(Y = 1|\mathbf{x}, \theta) \right)^2 dH(\mathbf{x}, \theta) \right] = O \left(B^{-\kappa/(\kappa+d)} \right),$$

for some $\kappa > 0$ and $d > 0$, where $H(\mathbf{x}, \theta)$ is a measure over $\mathcal{X} \times \Theta$.

Typically, κ relates to the smoothness of \mathbb{P} , while d relates to the number of covariates of the classifier — in our case, the number of parameters plus the number of features. Below, we provide some examples where Assumption 6 holds, using well-established results for the convergence rates of commonly used regression estimators:

- Kpotufe (2011) shows that kNN estimators are adaptive to the intrinsic dimension d under certain conditions. When $\widehat{\mathbb{P}}$ is a kNN estimator with \mathbb{P} in a class of Lipschitz continuous functions, Assumption 6 holds with $\kappa = 2$. More generally, with \mathbb{P} in a Hölder space with parameter $0 < \beta \leq 1.5$, Assumption 6 holds with $\kappa = 2\beta$ (Györfi et al. 2006; Ayano 2012).
- Kpotufe and Garg (2013) show that under certain conditions, when $\widehat{\mathbb{P}}$ is a kernel regression estimator with \mathbb{P} in a class of Lipschitz continuous functions, Assumption 6 holds with $\kappa = 2$ and d the intrinsic dimension of the data. More generally, with \mathbb{P} in a Hölder space with parameter $0 < \beta \leq 1.5$, Assumption 6 holds with $\kappa = 2\beta$ (Györfi et al. 2006).
- When $\widehat{\mathbb{P}}$ is a local polynomial regression estimator with \mathbb{P} in a Sobolev space with smoothness β , Assumption 6 holds with $\kappa = \beta$, where d is the manifold dimension (Bickel and Li 2007).
- Biau (2012) shows that under certain conditions, when $\widehat{\mathbb{P}}$ is a random forest estimator with D covariates with \mathbb{P} in a class of Lipschitz continuous functions, Assumption 6 holds with $\kappa = 2$ when the number of relevant features $d \leq D/2$.

More examples can be found in Györfi et al. (2006), Tsybakov (2009) and Devroye et al. (2013).

We also assume that the density of the product measure $G \times \pi$ is bounded away from infinity.

Assumption 7 (Bounded density) $H(\mathbf{x}, \theta)$ dominates $H' := G \times \pi$, and the density of H' with respect to H , denoted by h' , is such that there exists $\gamma > 0$ with $h'(\mathbf{x}, \theta) < \gamma$, $\forall \mathbf{x} \in \mathcal{X}, \theta \in \Theta$.

If the probabilistic classifier has the convergence rate given by Assumption 6, then the probability that hypothesis tests based on the BFF statistic versus the Bayes factor goes to zero has the rate given by the following theorem.

Theorem 4 *Under Assumptions 3-7, there exists $K'' > 0$ such that*

$$\mathbb{P}_{\mathcal{D}, \mathcal{T}|\theta}(\phi_{\tau}(\mathcal{D}) \neq \phi_{\widehat{\tau}_B}(\mathcal{D})) \leq 2\sqrt{K''}B^{-\kappa/(4(\kappa+d))}.$$

Corollary 2 tells us that the power of the BFF test is close to the power of the exact Bayes factor test. Because in the Neyman-Pearson setting the latter test is equivalent to the LRT, this implies that in this setting BFF converges to the most powerful test.

Corollary 2 *Under Assumptions 3-7, there exists $K'' > 0$ such that, for any $\theta \neq \theta_0$,*

$$\mathbb{P}_{\mathcal{D}, \mathcal{T}|\theta}(\phi_{\widehat{\tau}_B}(\mathcal{D}) = 1) \geq \mathbb{P}_{\mathcal{D}, \mathcal{T}|\theta}(\phi_{\tau}(\mathcal{D}) = 1) - 2\sqrt{K''}B^{-\kappa/(4(\kappa+d))}.$$

5. Sources of Error in LFI Confidence Sets

In traditional statistical inference, confidence sets depend on the choice of test statistic, the assumed distribution of the test statistic under the null, and the amount of available data. In LFI, however, there are additional sources of errors. For our LF2I inference machinery, we categorize these errors as follows:

- e_1 : Estimation error in learning the odds (Section 3.1);
- e_2 : Numerical error in evaluating the test statistic by maximization in **ACORE** (Equation 6) or by integration in **BFF** (Equation 8);
- e_3 : Estimation error in learning the critical values (Section 3.3.1) or the p-values (Section 3.3.2).

As shown in Section 4, validity is directly determined by e_3 . One can construct valid confidence sets regardless of how well the test statistics are estimated, as long as the quantile regression (Algorithm 1) or probabilistic classifier for estimating p-values (Algorithm 2) is consistent and the training sample size B' is large enough. The power or size of the confidence set is determined by both e_1 and e_2 . The error e_1 depends on the capacity of the classifier for estimating odds and the training sample size B . The error e_2 , on the other hand, is a purely numerical error and can be reduced by increasing the computational budget.

To mitigate all sources of errors, we use the following practical strategy:

- (A) First, select a probabilistic classifier and the sample size B for estimating odds based on the cross-entropy loss on held-out data;²
- (B) Then, choose the number of sampling points for computing the test statistic based on computational budget;
- (C) Finally, select the quantile regression (or probabilistic classifier for estimating p-values) and sample size B' to achieve nominal coverage across parameter space according to our diagnostics in Section 3.4 (the right branch in Figure 1).

6. Handling Nuisance Parameters

In most applications, only a small number of parameters in a model are of primary interest, with the other parameters then referred to as nuisance parameters. In this setting, the parameter space can be decomposed as $\Theta = \Phi \times \Psi$, where Φ contains the parameters of interest and Ψ contains nuisance parameters. The goal is to construct a confidence set for $\phi \in \Phi$. To guarantee frequentist coverage by Neyman's inversion technique, one needs to test null hypotheses of the form $H_{0,\phi_0} : \phi = \phi_0$ by comparing the test statistics to the cutoffs $\widehat{C}_{\phi_0} := \inf_{\psi \in \Psi} \widehat{C}_{(\phi_0, \psi)}$ (Section 3.3.1). That is, one needs to control the type I error

2. We note that one could also use the integrated odds loss (Equation 12) for step (A). However, as shown in Appendix F, the odds loss is much more sensitive than the cross-entropy loss to the value of the estimated odds, and can yield very large positive or negative values across different training sample sizes B .

at each ϕ_0 for *all* possible values of the nuisance parameters. Computing such infimum can be numerically unwieldy, especially if the number of nuisance parameters is large (van den Boom et al., 2020; Zhu et al., 2020).

In **ACORE**, we use a hybrid resampling or “likelihood profiling” method (Chuang and Lai, 2000; Feldman, 2000; Sen et al., 2009) to circumvent unwieldy numerical calculations as well as to reduce computational cost. For each ϕ , we first compute the “profiled” value

$$\hat{\psi}_\phi = \arg \max_{\psi \in \Psi} \prod_{i=1}^n \hat{\mathbb{O}}(\mathbf{X}_i^{\text{obs}}; (\phi, \psi)),$$

which (because of the odds estimation) is an approximation of the maximum likelihood estimate of ψ at the parameter value ϕ for observed data D . By definition, the estimated **ACORE** test statistic is exactly given by $\hat{\Lambda}(D; \phi_0) = \hat{\Lambda}(D; (\phi_0, \hat{\psi}_\phi))$. However, rather than comparing this statistic to \hat{C}_{ϕ_0} , we use the hybrid cutoff

$$\hat{C}'_{\phi_0} := \hat{F}^{-1}_{\hat{\Lambda}(D; \phi_0) | (\phi_0, \hat{\psi}_{\phi_0})}(\alpha), \quad (14)$$

where \hat{F}^{-1} is obtained via a quantile regression as in Algorithm 1, but using a training sample \mathcal{T}' generated at *fixed* $\hat{\psi}_{\phi_0}$. Alternatively, one can compute the p-value

$$\hat{p}(D; \phi_0) := \hat{\mathbb{P}}_{D | \mathcal{T}, \phi_0, \hat{\psi}_{\phi_0}} \left(\hat{\Lambda}(D; \phi_0) < \hat{\Lambda}(D; \phi_0) \right) \quad (15)$$

where $\hat{\mathbb{P}}$ is obtained via a regression as in Algorithm 2, but with \mathcal{T}' simulated at fixed $\hat{\psi}_{\phi_0}$. Hybrid methods do not always control α , but they are often a good approximation that lead to robust results (Aad et al., 2012; Qian et al., 2016). We refer to **ACORE** approaches based on Equation 14 or Equation 15 as “**h-ACORE**” approaches.

In contrast to **ACORE**, the **BFF** test statistic averages (rather than maximizes) over nuisance parameters. Hence, instead of adopting a hybrid resampling scheme to handle nuisance parameters, we approximate p-values and critical values, in what we refer to as “**h-BFF**”, by using the marginal model of the data \mathbf{X} at parameter of interest ϕ :

$$\tilde{f}(\mathbf{x} | \phi) = \int_{\nu \in \Psi} f_\theta(\mathbf{x}) d\pi(\nu).$$

We implement such a scheme by first drawing the train sample \mathcal{T}' from the entire parameter space $\Theta = \Phi \times \Psi$, and then applying quantile regression (or probabilistic classification) using ϕ only.

Algorithm 6 details our construction of **ACORE** and **BFF** confidence sets when calibrating critical values under the presence of nuisance parameter (construction via p-value estimation is analogous). In Section 7.3, we demonstrate how our diagnostics branch can shed light on whether or not the final results have adequate frequentist coverage.

7. Examples

Next, we analyze the empirical performance of our LF2I framework in different problem settings. We start in Section 7.1 with the Gaussian mixture model. This is a model where

the LR statistic is known but its null distribution is unknown, even asymptotically. Then, in Section 7.2, we assess how our procedures scale with parameter and feature dimension for the (analytically solvable) problem of estimating the population mean of d -dimensional Gaussian data. In Section 7.2.1, we first assume that the LR statistic is known but not its null distribution, so that we can compare our calibrated confidence sets to universal inference sets and the exact (uniformly most powerful) LR confidence sets. Thereafter, in Section 7.2.2, we consider the standard LFI setting with a likelihood that is only implicitly encoded by the simulator. Section 7.3 showcases our diagnostics, and compares the performance of h-ACORE, h-BFF and asymptotic chi-square results for an HEP example with nuisance parameters.

7.1 Gaussian Mixture Model Example: Unknown Null Distribution

It is challenging to construct valid confidence sets when sample sizes are small or the statistical model is irregular. In such situations, one cannot rely on the well-known χ^2 asymptotic behavior of the LR statistic (Drton, 2009). Nevertheless, a common practice in LFI is to first estimate the likelihood and then assume that the LR statistic is approximately χ^2 distributed. This can lead to invalid confidence sets with inadequate coverage. In addition, calibration can be difficult without efficient diagnostic tools.

The Gaussian mixture model (GMM) is a classical example where the (limiting) distribution of the LR statistic is intractable (Dacunha-Castelle and Gassiat, 1997), and where the development of valid statistical methods is an active area of research (Redner, 1981; McLachlan, 1987; Chen and Li, 2009; Wasserman et al., 2020). Here, we consider a one-dimensional normal mixture with unknown mean but known unit variance:

$$X \sim 0.5N(\theta, 1) + 0.5N(-\theta, 1).$$

Our goal is to construct a $1 - \alpha$ confidence set for the mean $\theta \in \Theta = [0, 5]$ given $n = 10$ observations of X . We can do so by inverting LR tests of the form $H_{0, \theta_0} : \theta = \theta_0$ for $\theta_0 \in \Theta$ as in Figure 2. The LR statistic is known for the mixture model, but not its null distribution or the critical values C_{θ_0} .

We compare three approaches for computing C_{θ_0} for the LR statistic (Equation 3):

- “LR with Monte Carlo samples”, where we estimate critical values at *fixed* θ_0 by drawing many Monte Carlo (MC) samples of size $n = 10$. Here, we generate 1000 MC samples at each point in a grid over Θ . The MC procedure is costly in practice, and does not scale with the dimension of the parameter space.
- “Chi-square LRT”, where we *assume* that $-2\text{LR}(\mathcal{D}; \theta_0) \sim \chi_1^2$, and hence take $-2C_{\theta_0}$ to be the same as the upper α quantile of a χ_1^2 distribution.
- “LR with calibrated C”, where we use Algorithm 1 with $B' = 1000$ simulations sampled uniformly on Θ to estimate C_{θ_0} across parameter space Θ via quantile regression.

Figure 3 shows diagnostics computed as in Section 3.4. Confidence sets from “Chi-square LRT” are clearly not valid. On the other hand, “LR with calibrated C” returns valid finite-sample confidence sets with coverage similar to “LR with Monte Carlo samples”.

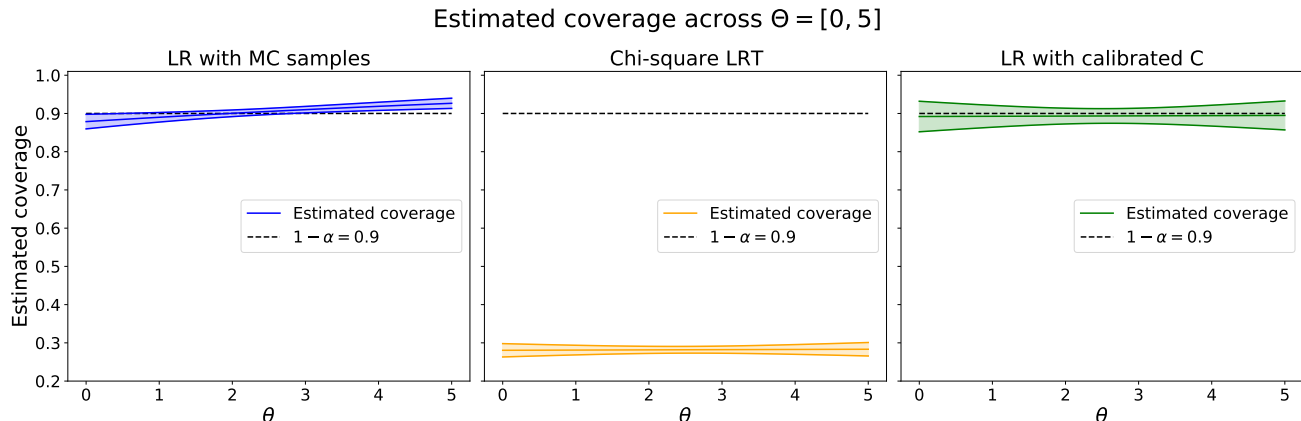


Figure 3: GMM example with $n = 10$. The plots show the estimated coverage (across the parameter space Θ) of 90% confidence sets for θ constructed with three different approaches; see text for details. We use the diagnostic branch of our LF2I framework with logistic regression to estimate empirical coverage; the plots shows the mean estimated coverage with two-standard-deviation ($\pm 2\sigma$) prediction intervals. *Left*: “LR with Monte Carlo samples” estimates the critical values C of the LR statistic by creating 1000 MC samples for each parameter value θ on a fine grid. This procedure is very costly, especially in higher dimensions. *Center*: “Chi-square LRT” assumes that the LR statistic has a χ^2 approximation. This approach clearly undercovers; confidence sets are not valid. *Right*: “LR with calibrated C ” uses Algorithm 1 (quantile regression with a total of $B' = 1000$ simulations) to find a parametrized function C_{θ_0} . Like “LR with Monte Carlo samples”, the construction returns finite-sample confidence sets with the nominal coverage of 0.9, but at a much lower cost.

7.2 Multivariate Gaussian Example: Scaling with Dimension

In this section, we investigate how our construction of frequentist confidence sets scales with the dimension of the parameter space. We ask: Do the confidence sets achieve the nominal coverage in practice for small sample sizes and reasonably large training sets? How does power depend on the dimension and the choice of test statistic (LR versus BF)? To provide clear benchmarks, we consider the well-studied problem of estimating the mean of a d -dimensional multivariate Gaussian (MVG) distribution. (This is an example where we can analytically derive test statistics as well as the exact null distribution of the LR statistic.)

Suppose $\mathbf{X}_1, \dots, \mathbf{X}_n \sim N(\theta, I_d)$, where I_d is the d -dimensional identity matrix and $\theta \in \mathbb{R}^d$ is an unknown parameter. For this model, the sample mean $\bar{\mathbf{X}}_n \sim N(\theta, n^{-1}I_d)$ is a sufficient statistic, so we can express our test statistics in terms of $\bar{\mathbf{X}}_n$. The likelihood ratio statistic for testing $H_{0,\theta_0} : \theta = \theta_0$ versus $H_{1,\theta_0} : \theta \neq \theta_0$ is

$$\text{LR}(\bar{\mathbf{X}}_n; \theta_0) = \log \frac{N(\bar{\mathbf{X}}_n; \theta_0, n^{-1}I_d)}{N(\bar{\mathbf{X}}_n; \bar{\mathbf{X}}_n, n^{-1}I_d)} = -\frac{n}{2} \|\bar{\mathbf{X}}_n - \theta_0\|^2. \quad (16)$$

For the MVG example, it holds exactly that $-2\text{LR}(\bar{\mathbf{X}}_n; \theta_0) \sim \chi_d^2$. We refer to inference based on the above result as “exact LRT”. For example, the exact LRT confidence set at level α is defined as

$$R^{\text{LRT}}(\bar{\mathbf{X}}_n) = \{\theta_0 \in \Theta : n\|\bar{\mathbf{X}}_n - \theta_0\|^2 \leq c_{\alpha,d}\},$$

where $c_{\alpha,d}$ is the upper α quantile of a χ_d^2 distribution.

For the Bayes factor, we assume a proposal distribution π that is uniform over an axis-aligned hyper-rectangle with corner points at $\mathbf{a} = (a, \dots, a)$ and $\mathbf{b} = (b, \dots, b) \in \mathbb{R}^d$ for $a < b$. The exact Bayes factor for testing $H_{0,\theta_0} : \theta = \theta_0$ versus $H_{1,\theta_0} : \theta \neq \theta_0$ is

$$\text{BF}(\bar{\mathbf{X}}_n; \theta_0) = \frac{N(\bar{\mathbf{X}}_n; \theta_0, n^{-1}I_d)}{\left(\frac{1}{b-a}\right)^d \prod_{j=1}^d \left[\frac{1}{2}\text{erf}\left(\frac{b-\bar{X}_{n,j}}{\sqrt{2n}}\right) - \frac{1}{2}\text{erf}\left(\frac{a-\bar{X}_{n,j}}{\sqrt{2n}}\right)\right]}. \quad (17)$$

(See Appendix F for a derivation.) We refer to inference based on the above expression and high-resolution Monte Carlo sampling to compute critical values as “exact BF”.

With exact LRT and exact BF as benchmarks, we assess the coverage and power of our LFI constructed confidence sets with increasing parameter and feature dimension d . We study two cases of LFI with intractable distributions. In Section 7.2.1, we assume that we know the LR statistic (Equation 16), but not its null distribution or critical values. In Section 7.2.2, we consider the more challenging LFI scenario where one is only able to sample data from a forward simulator F_θ , and hence needs to estimate both the test statistic and critical values.

7.2.1 FINITE-SAMPLE CONFIDENCE SETS FOR KNOWN TEST STATISTIC

First, we consider the LFI case where the test statistic is known, but not its null distribution and critical values. Such a situation may arise when the the sample size is small or when the LR statistic does not have a known asymptotic behavior (as for mixture models, Drton 2009). Recently, Wasserman et al. (2020) proposed a general set of procedures for constructing confidence sets and hypothesis tests with finite-sample guarantees. One instance of universal inference uses the crossfit likelihood-ratio test (crossfit LRT), which averages the likelihood ratio statistic over two data splits. Our LFI approach can also produce valid finite-sample confidence sets for known test statistic by calibrating the critical value as in Algorithm 1.

Figure 4 compares three “Exact LRT” sets with confidence sets constructed with our method for estimating the critical value (“LR with calibrated C”), and confidence sets via universal inference (“Crossfit LRT”). The dimension here is $d = 2$, the true parameter is $\theta = (0, 0)$, and the sample size is $n = 10$. By calibrating the critical value, we can achieve valid confidence sets similar to exact LRT for a modest number of $B' = 500$ simulations. Universal inference does not adjust the critical values according to the value of θ , and pays a price for its generality in terms of larger confidence sets and lower power.

Figure 5 extends the comparison to coverage and power in higher dimensions d . As before, we observe a sample of size $n = 10$ from a MVG centered at $\theta = \mathbf{0}$. We construct confidence sets using exact LRT, LR with calibrated C, and crossfit LRT for 100 draws from the MVG. We then test $H_{0,\theta_0} : \theta = \theta_0$ versus $H_{1,\theta_0} : \theta \neq \theta_0$ for different values

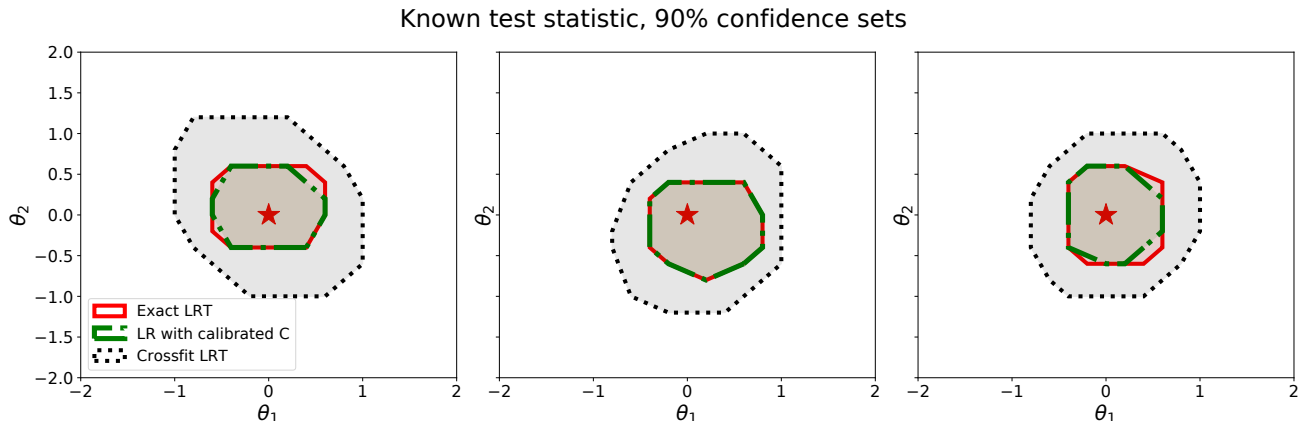


Figure 4: Confidence sets for known test statistics and bivariate Gaussian data. When $d = 2$, our method for estimating critical values with $B' = 500$ simulations (“LR with calibrated C”; green contour) returns 90% confidence sets that are close to the exact LRT confidence sets (red contour) and smaller than the more conservative universal via crossfit LRT sets (gray shading). The figures correspond to three random realizations of observed data with $n = 10$ drawn from the Gaussian model with true parameter $\theta = (0, 0)$ (indicated with a red star).

of θ_0 at increasing distance $\|\theta_0\|$ from the origin. We reject H_{0,θ_0} if θ_0 is outside the constructed confidence set. In this example, coverage is measured by the proportion of times the parameter value $\theta_0 = \mathbf{0}$ is (correctly) included in the confidence set over 100 such repetitions. Similarly, power is measured by the proportion of times a parameter value $\theta_0 \neq \mathbf{0}$ is (correctly) outside the constructed confidence set. For better visualization, we have chosen the test points θ_0 so that we have roughly an equal number of test points at each squared distance $\|\theta_0\|^2$.

The table at the top of the figure shows that both “LR with calibrated C” and “Crossfit LRT” control the type I error at level $\alpha = 0.1$ for dimensions d between 10 to 100. Crossfit LRT, however, tends to be overly conservative. As for the two-dimensional example, our method achieves almost the same power as the exact LR test, even for $d = 100$ and a modest budget of $B' = 5000$ simulations. Crossfit LRT has much lower power, as expected. The differences in power between the two methods grows with increasing dimension d .

7.2.2 FINITE-SAMPLE CONFIDENCE SETS IN AN LFI SETTING

Next, we consider the more challenging LFI scenario where one is only able to sample data from a forward simulator F_θ . As before, we simulate observed data of sample size $n = 10$ from a d -dimensional Gaussian distribution with true mean $\theta^* = \mathbf{0}$, but now we estimate both the test statistics and the critical values for controlling the type I error. We use **ACORE** to approximate the LRT, and **BFF** to approximate tests based on the Bayes factor with a uniform prior over the hyper-rectangle $[-5, 5]^d$.

Finite-sample confidence sets for known test statistic

	d=10	d=20	d=50	d=100
Coverage of LR with calibrated C	0.91 ± 0.03	0.91 ± 0.03	0.88 ± 0.03	0.88 ± 0.03
Coverage of crossfit LRT	0.993 ± 0.008	0.997 ± 0.005	1.000 ± 0.000	1.000 ± 0.000

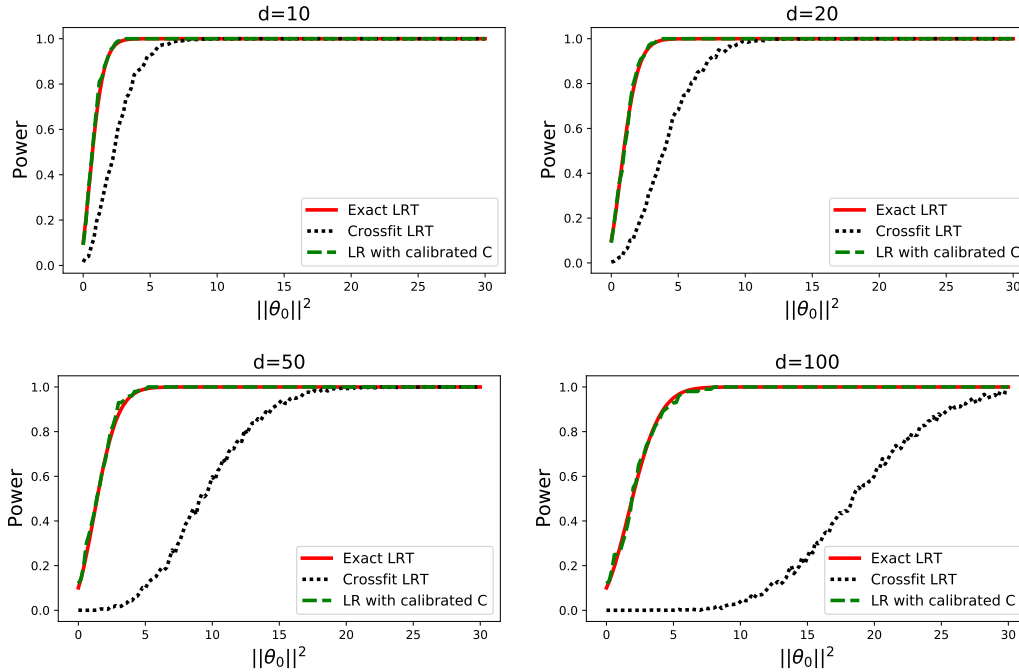


Figure 5: Confidence sets for known test statistic and d -dimensional Gaussian data. Coverage and power of finite-sample confidence sets constructed via exact LRT, LR with calibrated C, and universal inference via crossfit LRT (see text for details). All methods achieve the nominal coverage of 0.9. When the likelihood ratio statistic is known, our construction with $B' = 5000$ simulations yields the same power as the exact LRT, even in high dimensions. By calibrating the critical values, one can achieve more precise confidence sets and higher power than universal inference. See Figure 4 for example confidence sets in dimension $d = 2$. The difference in precision and power between the two methods increase with dimension d .

Following the strategy outlined in Section 5, we select a quadratic discriminant analysis (QDA) classifier to estimate the odds, and quantile regression with gradient boosted trees to estimate cutoffs at level $\alpha = 0.1$. Figure 6 compares ACORE and BFF confidence sets when $d = 2$ to the exact LRT and exact BF counterparts (achieved with computationally expensive MC sampling to estimate critical values). Both ACORE and BFF achieve similarly sized confidence sets as their exact counterparts, with modest budgets of $B = B' = 5000$ simulations and $M = 2500$ evaluation points for maximization or integration.

Figure 7 shows the coverage and power of these methods as the dimension d increases. We use the same approach as in Section 7.2.1 to compute the power over 100 repetitions. First, we observe that both ACORE and BFF confidence sets consistently achieve the nom-

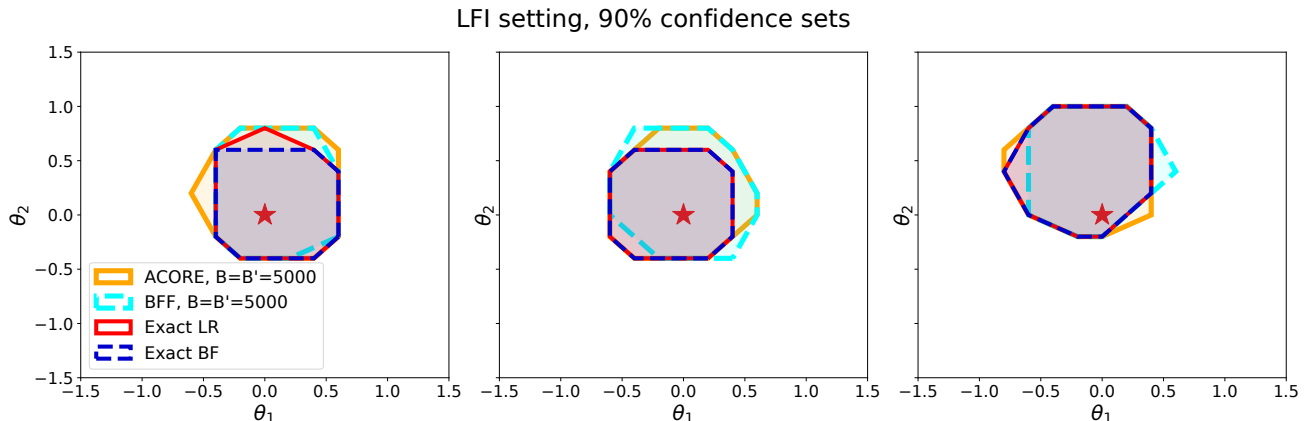


Figure 6: LFI setting: When $d = 2$, BFF and ACORE 90% confidence sets are of similar size to those constructed using the exact LR and BF. The true parameter $\theta = (0, 0)$ (indicated with a star), $n = 10$ observations, $B = B' = 5000$ and $M = 2500$ samples for BFF and ACORE. The figures show three random realizations of the observed data.

inal 0.90 confidence level,³ even in higher dimensions. Next, we consider power. Loosely speaking, the exact LRT and BF power curves can be seen as upper bounds on the power of ACORE and BFF, respectively. The results indicate that ACORE and BFF confidence sets are precise in low dimensions, but their power drops as d increases.

A closer look (see Appendix F) indicates that the loss in power for $d \geq 5$ is primarily due to numerical error in the maximization or integration step (referred to as error e_2 in Section 5) of ACORE and BFF, respectively. Hence, we foresee that the current implementations of ACORE and BFF with uniformly spaced evaluation points would significantly benefit from more efficient numerical computation. For maximization, higher efficiency approaches have been suggested in the hyper-parameter search literature for machine learning algorithms, such as kernel-based Bayesian optimization (Kandasamy et al., 2015) and bandit-based approaches (Li et al., 2018) (see Feurer and Hutter (2019) for an overview). For integration, one could employ more efficient approaches that rely on, e.g., adaptive sampling (Peter Lepage, 1978; Jadach, 2003), nested sampling (Feroz et al., 2009; Handley et al., 2015) or machine learning algorithms (Bendavid, 2017; Gao et al., 2020).

7.3 High-Energy Physics Example: Nuisance Parameters

Hybrid methods, which maximize or average over nuisance parameters, do not always control the type I error of statistical tests. For small sample sizes, there is no theorem as to whether profiling or marginalization of nuisance parameters will give better frequentist coverage for the parameter of interest (Cousins, 2018, Section 12.5.1). In addition, most practitioners consider a thorough check of frequentist coverage to be impractical (Cousins, 2018, Section 13). In this example, we apply the LFI hybrid schemes from Section 6 to a high-energy

3. The coverage falls within or above expected variation for 100 repetitions, which is in the range [84, 95].

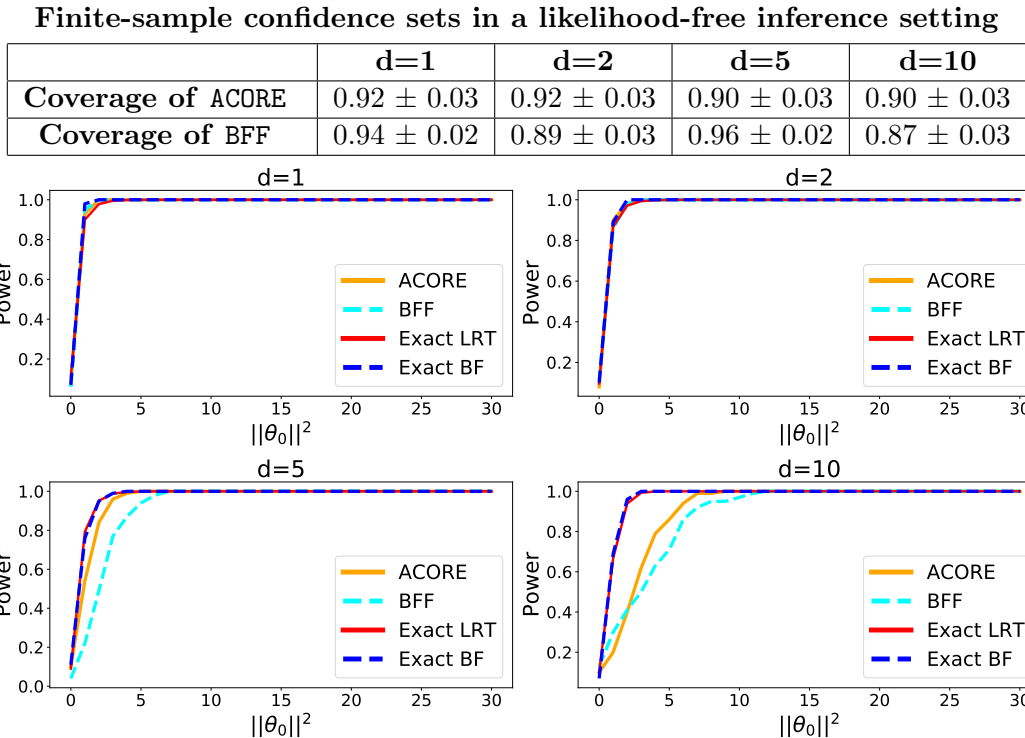


Figure 7: LFI setting: Coverage and power for ACORE and BFF confidence sets and their exact likelihood ratio test (LRT) and Bayes factor (BF) counterparts at dimension $d = 1, 2, 5$ and 10 across 100 repetitions. Both ACORE and BFF return valid confidence sets with coverage at or above the nominal confidence level $1 - \alpha = 0.9$. The loss in power relative the exact methods increases as d increases. (We use QDA to learn the odds, with sample size B guided by Figure 10, a computational budget for maximization and integration of $M = 10000$, and quantile regression gradient boosting trees with $B' = 10000$.)

physics (HEP) counting experiment (Lyons, 2008; Cowan et al., 2011; Cowan, 2012) with nuisance parameters. We illustrate how our diagnostics can guide the analyst and provide insight into which method to choose for the problem at hand.

Consider a ‘‘Poisson counting experiment’’ where particle collision events are counted under the presence of both an uncertain background process and a (new) signal process. The goal is to estimate the signal strength. To avoid identifiability issues, the background rate is estimated separately by counting the number of events in a control region where the signal is believed to be absent. Hence, the observable data $\mathbf{X} = (M, N)$ contain two measurements, where $M \sim \text{Pois}(\gamma b)$ is the number of events in the control region, and $N \sim \text{Pois}(b + \epsilon \cdot s)$ is the number of events in the signal region. Our parameter of interest is the signal strength s , and we will treat b and ϵ as nuisance parameters. (The parameter ϵ is a factor for the number of signal events expected in a particular experiment; it can, for instance, represent experimental inefficiencies or the experiment’s running time (Lyons, 2008). The parameter γ is a scaling parameter that we take here as known.) In our example, we set $\gamma = 1$ and

assume $n = 10$ observations from the Poisson model above, with parameters in the ranges $s \in [0, 20]$, $b \in [90, 110]$ and $\epsilon \in [0.5, 1.0]$.

Figure 8, top, shows examples of 90% confidence sets for the signal strength s for observed data with true parameter $\theta^* = (s^*, b^*, \epsilon^*) = (10, 100, 0.75)$. (We learn the odds using a QDA classifier with $B = 100000$; $n = 10$, $B' = 10000$ and $M = 10000$.) The table lists the estimated coverage $\widehat{\mathbb{P}}_{\mathcal{D}|\theta^*}(\theta^* \in \widehat{R}(\mathcal{D}))$ for 100 repetitions at θ^* . The box plots show the distribution of confidence set lengths as a percentage of the signal parameter range $[0, 20]$ for the same 100 repetitions. In our comparison, we include h-ACORE and h-BFF confidence intervals, which we construct with the critical value and p-value hybrid schemes in Algorithm 6. We also include ACORE confidence intervals with cutoffs derived from the χ^2 distribution (which is the asymptotic distribution of the profiled likelihood ratio; Murphy and Van Der Vaart 2000). These results seem to imply that all five methods return valid confidence intervals, with the intervals based on calibrated critical values or p-values being shorter (more powerful) than those for ACORE based on asymptotic cutoff. Furthermore, h-BFF confidence sets appear to be shorter and less variable than h-ACORE confidence sets. Figure 8, however, only considers confidence sets for data at a particular θ -value. Next, we showcase how our diagnostic branch (Section 3.4) allows for a more thorough analysis of coverage over the entire parameter space.

With logistic regression and a total of $B'' = 500$ simulations, we compute the estimated coverage with a two-standard-deviation prediction band for all $\theta = (s, b, \epsilon)$ over a regular grid across the parameter space Θ . Parameter regions where the nominal coverage of $1 - \alpha = 0.9$ falls within the prediction band are considered to have “correct coverage” (CC). Regions where the upper versus lower limit of the prediction band falls below versus above $1 - \alpha$ are labeled as having “undercoverage” (UC) and “overcoverage” (OC), respectively. Figure 9, top, highlights that a very small portion (4.0%) of the parameter space has undercoverage for the hybrid version of BFF, whereas the ACORE approach based on asymptotic cutoff overcovers for all parameter values. The middle panel shows exactly where the CC, UC and OC regions fall in parameter space for the three different approaches; the bottom panel displays the values of the upper limit of the prediction band for coverage. Interestingly, these results illustrate that h-BFF, which averages over nuisance parameters, has the best overall performance, but it can severely undercover for a small region with low ϵ , low background b and high signal s . On the other hand, h-ACORE based on hybrid resampling undercovers (but only slightly) in a larger region of the parameter space with high ϵ , small signal s and high background b .

Often, coverage is evaluated using analyses similar to Figure 8 for best-fit or fiducial parameter values. Figure 9 is an example of how our LF2I framework can provide the analyst with a more complete and interpretable check of validity.

8. Conclusions and Discussion

Validity. Our proposed LF2I methodology leads to frequentist confidence sets and hypothesis tests with finite-sample guarantees (when there are no nuisance parameters). *Any* existing or new test statistic — that is, not only estimates of the LR statistic — can be plugged into our framework to create tests that indeed control type I error. The implicit assumption is that the null distribution of the test statistic varies smoothly in parameter

HEP example with nuisance parameters

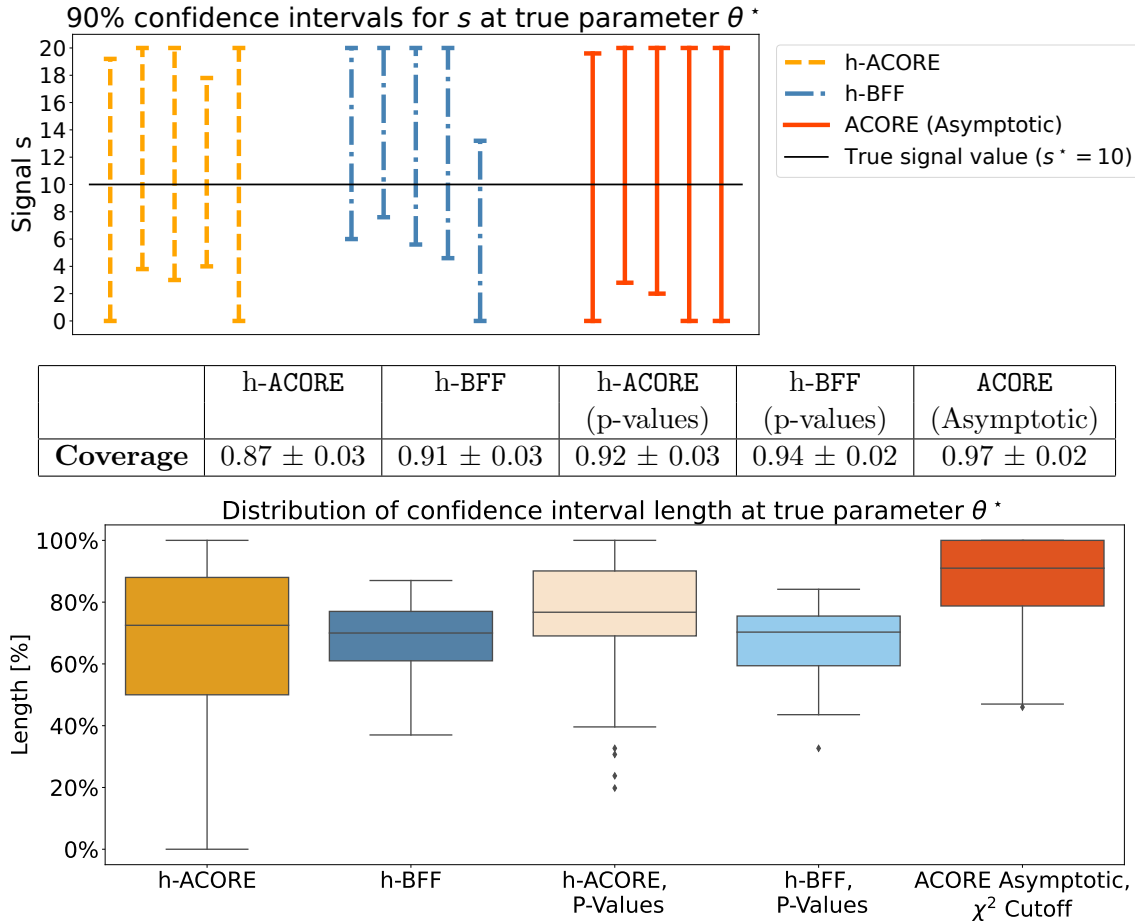


Figure 8: HEP example with nuisance parameters. *Top*: Examples of 90% confidence intervals of the signal strength s for observed data $X^{obs} = (X_1, \dots, X_{10})$ from a model with true parameter $\theta^* = (s^*, b^*, \epsilon^*)$. *Center/bottom*: Repeat the construction of confidence intervals 100 times for data simulated at θ^* . The table lists the estimated coverage, and the boxplots graph the distribution of the length of constructed confidence intervals (as a percentage of the total parameter range for s). While all LFI methods appear to construct valid confidence intervals, calibration of critical values and p-values (with BFF, in particular) lead to smaller and more powerful confidence intervals.

space. If that condition holds, then we can efficiently leverage quantile regression methods to construct valid confidence sets by a Neyman inversion of simple hypothesis tests, without having to rely on asymptotic results. In settings where the likelihood can be evaluated, our framework leads to more powerful tests and smaller confidence sets than universal inference, but at the cost of having to simulate data from the likelihood.

Nuisance parameters and diagnostics. For small sample sizes, there is no theorem to tell us whether profiling or marginalization of nuisance parameters will give better frequen-

Diagnostics for HEP example with nuisance parameters

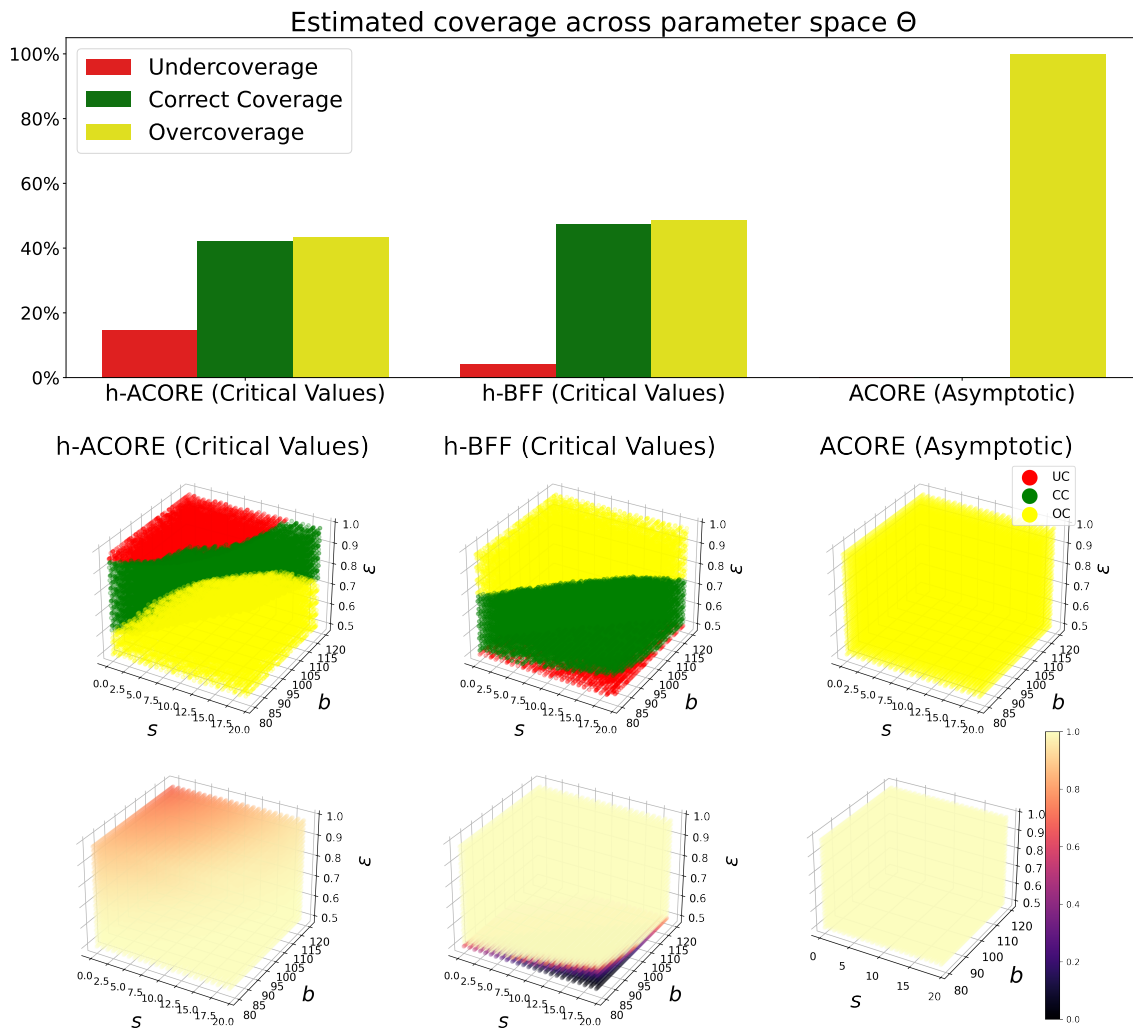


Figure 9: Hybrid approaches which maximize or average over nuisance parameters do not guarantee frequentist coverage. Our diagnostic tool (Section 3.4) can identify regions in parameter space with undercoverage (UC), correct coverage (CC), and overcoverage (OC), respectively. See text for details. *Top*: h-BFF performs the best in terms of having the largest proportion of the parameter space with correct coverage and only a small fraction of the parameter space with undercoverage. *Center*: Points in parameter space colored by label (UC, CC, OC). *Bottom*: Points in parameter space colored by the upper limit of the two-standard-deviation prediction interval for coverage. The latter results reveal that h-BFF with averaging over nuisance parameters tends to undercover more severely (though in a very small region of the parameter space) than h-ACORE with critical values via hybrid resampling/profiling; the UC regions of h-BFF here correspond to settings with low ϵ , high s and low b .

tist coverage for the parameter of interest (Cousins, 2018, Section 12.5.1). It is generally believed that hybrid resampling methods return approximately valid confidence sets, but that a rigorous check of validity is infeasible when the true solution is not known. Our diagnostic branch presents practical tools for assessing empirical coverage across the entire parameter space (including nuisance parameters). After the data scientist sees the results, he/she can decide which method is most appropriate for the application at hand. For example, in our HEP counting experiment (Section 7.3), our diagnostics revealed that h-BFF (which averages the estimated odds over nuisance parameters) returned less variable results and higher power in an LFI setting, but with small regions of the parameter space under-covering more severely than h-ACORE (which maximizes the estimated odds over nuisance parameters).

Power. Statistical power is the hardest property to achieve in practice in LFI. This is the area where we foresee that most statistical and computational advances will take place. As mentioned in Section 5 and then illustrated in Section 7.2.2, the power or size of the LFI confidence sets for θ depends not only on the theoretical properties of the (exact) test statistics, such as the LR statistic or the Bayes factor. Ultimately, the power may be decided by: (1) how well we are able to estimate the likelihood or odds (this is the e_1 statistical estimation error), and (2) how accurately we, in practice, compute the target test statistic by integration or maximization (this is the e_2 numerical error). Machine learning offers exciting possibilities on both fronts. For example, with regards to (1), Brehmer et al. (2020b) offer compelling evidence that one can dramatically improve estimates of the likelihood $p(\mathbf{x}|\theta)$ for $\theta \in \Theta$, or the likelihood ratio $p(\mathbf{x}|\theta_1, \theta_2)$ for $\theta_1, \theta_2 \in \Theta$, by a “mining gold” approach that extracts additional information from the simulator about the latent process. Future work could incorporate a mining gold approach into our general LF2I framework, with the calibration and diagnostic branches as separate modules. This might improve estimates of the odds $\mathbb{O}(\mathbf{X}; \theta)$ (Equation 5), and thereby likelihood-based test statistics such as ACORE and BFF.

Other test statistics. Our work also presents another new direction for likelihood-free frequentist inference: So far frequentist LFI methods are estimating either likelihoods or likelihood ratios, and then often relying on asymptotic properties of the LR statistic. We note that there are settings where it may be easier to estimate the posterior $p(\theta|\mathbf{x})$ than the likelihood $p(\mathbf{x}|\theta)$; the same way there may be settings where the Bayes factor in practice leads to higher power than the LRT. Because our general LF2I framework (for creating valid finite-sample confidence sets and tests) is agnostic to whether we use Bayesian or classical algorithms to create the test statistic itself, we can potentially leverage prediction methods that estimate the conditional mean $\mathbb{E}[\theta|\mathbf{x}]$ and variance $\mathbb{V}[\theta|\mathbf{x}]$ to construct frequentist confidence sets and hypothesis tests for θ with finite-sample guarantees. We are currently exploring the test statistic $T = \frac{(\mathbb{E}[\theta|\mathbf{x}] - \theta_0)^2}{\mathbb{V}[\theta|\mathbf{x}]}$ (private communication with Luca Masserano, June 2021), which in some scenarios corresponds to the Wald statistic for testing $H_{0, \theta_0} : \theta = \theta_0$ against $H_{1, \theta_0} : \theta \neq \theta_0$ (Wald, 1943), as a potentially more attractive alternative to the LR statistic.

Acknowledgments

The authors would like to thank Mikael Kuusela, Rafael Stern and Larry Wasserman for helpful discussions. This work was supported in part by NSF DMS-2053804, NSF PHY-2020295, and the C3.ai Digital Transformation Institute. RI is grateful for the financial support of CNPq (309607/2020-5) and FAPESP (2019/11321-9).

Appendix A. Estimating Odds

Algorithm 3 provides details on how to create the training sample \mathcal{T} for estimating odds. Out of the total training sample size B , a proportion p is generated by the stochastic forward simulator F_θ at different parameter values θ , while the rest is sampled from a reference distribution G . Note that G can be any distribution that dominates F_θ . If G is the marginal distribution $F_{\mathbf{X}}$ and the observed sample size is $n = 1$, then the denominator of the BFF statistic is exactly equal to one, allowing us to bypass the calculation of the denominator.

Algorithm 3 Generate a labeled sample of size B for estimating odds

Require: stochastic forward simulator F_θ ; reference distribution G ; proposal distribution π_Θ over parameter space; training sample size B for estimating the odds; parameter p of Bernoulli distribution

Ensure: labeled training sample

```

1: Set  $\mathcal{T} \leftarrow \emptyset$ 
2: for  $i$  in  $\{1, \dots, B\}$  do
3:   Draw parameter value  $\theta_i \sim \pi_\Theta$ 
4:   Draw  $Y_i \sim \text{Ber}(p)$ 
5:   if  $Y_i == 1$  then
6:     Draw sample  $\mathbf{X}_i \sim F_{\theta_i}$ 
7:   else
8:     Draw sample  $\mathbf{X}_i \sim G$ 
9:   end if
10:   $\mathcal{T} \leftarrow \mathcal{T} \cup (\theta_i, \mathbf{X}_i, Y_i)$ 
11: end for
12: return  $\mathcal{T} = \{\theta_i, \mathbf{X}_i, Y_i\}_{i=1}^B$ 

```

Algorithm 4 Sample from the marginal distribution $F_{\mathbf{X}}$

Require: stochastic forward simulator F_θ ; proposal distribution π_Θ over parameter space

Ensure: sample \mathbf{X}_i from the marginal distribution $F_{\mathbf{X}}$

```

1: Draw parameter value  $\theta_i \sim \pi_\Theta$ 
2: Draw sample  $\mathbf{X}_i \sim F_{\theta_i}$ 
3: return  $\mathbf{X}_i$ 

```

Appendix B. Estimating Empirical Coverage Across the Parameter Space

Algorithm 5 provides details on our “local” goodness-of-fit procedure (the diagnostics branch in Figure 2), which estimates the empirical coverage $\mathbb{P}_{\mathcal{D}|\theta}(\theta \in \widehat{R}(\mathcal{D}))$ as a continuous function of $\theta \in \Theta$. Our procedure is to first draw B'' new samples from the simulator to generate synthetic data $\mathcal{T}'' = \{(\theta'_1, \mathcal{D}'_1), \dots, (\theta'_{B''}, \mathcal{D}'_{B''})\}$, where $\theta'_i \sim \pi_\Theta$ and $\mathcal{D}'_i := \{\mathbf{X}_{i,1}, \dots, \mathbf{X}_{i,n}\} \stackrel{\text{iid}}{\sim} F_{\theta'_i}$. For each sample \mathcal{D}'_i , we then check whether or not the test statistic λ_i is larger than the estimated critical value $\widehat{C}_{\theta'_i}$ (the output from Algorithm 1);

this is equivalent to computing a binary variable W_i for whether or not the “true” value θ'_i falls within the confidence set $\widehat{R}(\mathcal{D}'_i)$ (Equation 10). Note that the computations of the test statistic and the critical value are amortized, meaning that we do not retrain algorithms to estimate these two quantities.

The final step in our diagnostic branch is to use a probabilistic classifier to smoothly estimate empirical coverage as a function of θ by regressing W on θ' . This estimation requires a new fit, but after training the probabilistic classifier, we can evaluate the estimated coverage anywhere in parameter space Θ .

Algorithm 5 Estimate the empirical coverage $\mathbb{P}_{\mathcal{D}|\theta}(\theta \in \widehat{R}(\mathcal{D}))$, for all $\theta \in \Theta$ simultaneously.

Require: stochastic forward simulator F_θ ; π_Θ (a fixed proposal distribution over the full parameter space Θ); sample size B'' for estimating coverage; test statistic λ ; nominal coverage α ; estimated critical values \widehat{C}_θ ; regression estimator m

Ensure: estimated coverage $\widehat{\mathbb{P}}_{\mathcal{D}|\theta}(\theta \in \widehat{R}(\mathcal{D}))$ for all $\theta \in \Theta$, where \widehat{R} is the region derived from λ and \widehat{C}_θ (Equation 10)

- 1: Set $\mathcal{T}'' \leftarrow \emptyset$
 - 2: **for** i in $\{1, \dots, B''\}$ **do**
 - 3: Draw parameter $\theta'_i \sim \pi_\Theta$
 - 4: Draw sample $\mathcal{D}'_i := \{\mathbf{X}_{i,1}, \dots, \mathbf{X}_{i,n}\} \stackrel{iid}{\sim} F_{\theta'_i}$
 - 5: Compute test statistic $\lambda_i \leftarrow \lambda(\mathcal{D}'_i; \theta'_i)$
 - 6: Compute indicator variable $W_i \leftarrow \mathbb{I}(\lambda_i \geq \widehat{C}_{\theta'_i})$
 - 7: $\mathcal{T}'' \leftarrow \mathcal{T}'' \cup \{(\theta'_i, W_i)\}$
 - 8: **end for**
 - 9: Use \mathcal{T}'' to learn parametrized function $\widehat{\mathbb{P}}_{\mathcal{D}|\theta}(\theta \in \widehat{R}(\mathcal{D}))$ by regressing W on θ'
 - 10:
 - 11: **return** $\widehat{\mathbb{P}}_{\mathcal{D}|\theta}(\theta \in \widehat{R}(\mathcal{D}))$
-

Appendix C. Constructing Confidence Sets Under the Presence of Nuisance Parameters

Algorithm 6 provides details on how to construct **ACORE** and **BFF** confidence sets when calibrating critical values with nuisance parameters present (the algorithm based on p-value estimation is analogous). Note that the first chunk on estimating the odds and the last chunk with Neyman inversion are the same for **ACORE** and **BFF**. Furthermore, the test statistics are the same whether or not there are nuisance parameters.

Algorithm 6 Construct confidence set for ϕ with coverage $1 - \alpha$ by calibrating critical values (under the presence of nuisance parameters)

Require: stochastic forward simulator F_θ ; proposal distribution π over $\Theta = \Phi \times \Psi$; parameter p of Bernoulli distribution; sample size B (for estimating odds ratios); sample size B' (for estimating critical values or p-values); probabilistic classifier; observed data $D = \{\mathbf{x}_1^{\text{obs}}, \dots, \mathbf{x}_n^{\text{obs}}\}$; desired level $\alpha \in (0, 1)$; number of parameter values at which to evaluate confidence set, n_{grid} ; test statistic `test_stat` (ACORE or BFF)

Ensure: ϕ -values in confidence set

- 1: // **Estimate odds**
- 2: Generate labeled sample \mathcal{T} according to Algorithm 3
- 3: Apply probabilistic classifier to \mathcal{T} to learn $\widehat{\mathbb{P}}(Y = 1|\theta, \mathbf{X})$, for all $\theta = (\phi, \psi) \in \Theta$ and $\mathbf{X} \in \mathcal{X}$
- 4: Let the estimated odds $\widehat{\mathcal{O}}(\mathbf{X}; \theta) \leftarrow \frac{\widehat{\mathbb{P}}(Y=1|\theta, \mathbf{X})}{\widehat{\mathbb{P}}(Y=0|\theta, \mathbf{X})}$
- 5: // **Compute (hybrid) cut-offs for (h-)ACORE or (h-)BFF**
- 6: **if** `test_stat` == ACORE **then**
- 7: Define $\widehat{\psi}_\phi \leftarrow \arg \max_{\psi \in \Psi} \prod_{i=1}^n \widehat{\mathcal{O}}(\mathbf{x}_i^{\text{obs}}; (\phi, \psi))$ for every ϕ
- 8: Define the test statistic $\lambda(\mathcal{D}; \phi) \leftarrow \widehat{\Lambda}(\mathcal{D}; (\phi, \widehat{\psi}_\phi))$, for every ϕ , to be the ACORE statistic (Equation 6) with estimated odds
- 9: Apply quantile regression to \mathcal{T} to learn $\widehat{C}_\phi = \widehat{F}_{\lambda(\mathcal{D}; \phi)|(\phi, \widehat{\psi}_\phi)}^{-1}(\alpha)$ for every ϕ
- 10: **else if** `test_stat` == BFF **then**
- 11: Define $\pi_\Psi(\psi) \leftarrow$ restriction of proposal distribution π over Ψ
- 12: Define the test statistic $\lambda(\mathcal{D}; \phi) \leftarrow \widehat{\tau}(\mathcal{D}; \phi) := \frac{\int_\Psi \prod_{i=1}^n \widehat{\mathcal{O}}(\mathbf{x}_i^{\text{obs}}; (\phi, \psi)) d\pi_\Psi(\psi)}{\int_\Theta \prod_{i=1}^n \widehat{\mathcal{O}}(\mathbf{x}_i^{\text{obs}}; \theta) d\pi_1(\theta)}$, for every ϕ , to be the BFF statistic (Equation 8) with estimated odds
- 13: Apply quantile regression to \mathcal{T} to learn $\widehat{C}_\phi = \widehat{F}_{\lambda(\mathcal{D}; \phi)|(\phi)}^{-1}(\alpha)$
- 14: **end if**
- 15: // **Confidence sets for ϕ via Neyman inversion**
- 16: Initialize confidence set $\widehat{R}(D) \leftarrow \emptyset$
- 17: Let $L_\Phi \leftarrow$ lattice over Φ with n_{grid} elements
- 18: **for** $\phi_0 \in L_\Phi$ **do**
- 19: **if** $\lambda(D; \phi_0) > \widehat{C}_{\phi_0}$ **then**
- 20: Add ϕ_0 to the confidence set $\widehat{R}(D) \leftarrow \widehat{R}(D) \cup \{\phi_0\}$
- 21: **end if**
- 22: **end for**
- 23: **return** confidence set $\widehat{R}(D)$

Appendix D. Theoretical Guarantees for ACORE with Calibrated Critical Values

We start by showing that our procedure for choosing critical values leads to valid hypothesis tests (that is, tests that control the type I error probability) as long as B' in Algorithm 1 is large enough. In order to do so, we assume that the quantile regression estimator described in Section 3.3.1 is consistent in the following sense:

Assumption 8 Let $\widehat{F}_{B'}(\cdot|\theta)$ be the estimated cumulative distribution function of the test statistic $\lambda(\mathcal{D}; \Theta_0)$ conditional on θ based on a sample \mathcal{T} with size B' , and let $F(\cdot|\theta)$ be its true conditional distribution. For every $\theta \in \Theta_0$, assume that the quantile regression estimator is such that

$$\sup_{\lambda \in \mathbb{R}} |\widehat{F}_{B'}(\lambda|\theta) - F(\lambda|\theta)| \xrightarrow[B' \rightarrow \infty]{\mathbb{P}} 0.$$

Assumption 8 holds, for instance, for quantile regression forests (Meinshausen, 2006).

Next, we show that Algorithm 1 yields a valid hypothesis test as $B' \rightarrow \infty$.

Theorem 5 Let $C_{B'} \in \mathbb{R}$ be the critical value of the test based on the statistic $\lambda(\mathcal{D}; \Theta_0)$ chosen according to Algorithm 1 for a fixed $\alpha \in (0, 1)$. If the quantile estimator satisfies Assumption 8 and either

- $|\Theta| < \infty$,
- Θ is a compact subset of \mathbb{R}^d , and the function $g_{B'}(\theta) = \sup_{t \in \mathbb{R}} |F_{B'}(t|\theta) - F(t|\theta)|$ is continuous in θ and strictly decreasing in B' ,

then

$$C_{B'} \xrightarrow[B' \rightarrow \infty]{\mathbb{P}} C^*,$$

where C^* is such that

$$\sup_{\theta \in \Theta_0} \mathbb{P}_{\mathcal{D}|\theta}(\lambda(\mathcal{D}; \Theta_0) \leq C^*) = \alpha.$$

Proof If $|\Theta| < \infty$, the union bound and Assumption 8 imply that

$$\sup_{\theta \in \Theta_0} \sup_{\lambda \in \mathbb{R}} |\widehat{F}_{B'}(\lambda|\theta) - F(\lambda|\theta)| \xrightarrow[B' \rightarrow \infty]{\mathbb{P}} 0. \quad (18)$$

Similarly, by Dini's theorem, Equation 18 also holds if Θ is a compact subset of \mathbb{R}^d , and the function $g_{B'}(\theta)$ is continuous in θ and strictly decreasing in B' . It follows that

$$\sup_{\theta \in \Theta_0} |\widehat{F}_{B'}^{-1}(\alpha|\theta) - F^{-1}(\alpha|\theta)| \xrightarrow[B' \rightarrow \infty]{\mathbb{P}} 0.$$

The result follows from the fact that

$$\begin{aligned} 0 \leq |C_{B'} - C^*| &= \left| \sup_{\theta \in \Theta_0} \widehat{F}_{B'}^{-1}(\alpha|\theta) - \sup_{\theta \in \Theta_0} F^{-1}(\alpha|\theta) \right| \\ &\leq \sup_{\theta \in \Theta_0} |\widehat{F}_{B'}^{-1}(\alpha|\theta) - F^{-1}(\alpha|\theta)|, \end{aligned}$$

and thus

$$|C_{B'} - C^*| \xrightarrow[B' \rightarrow \infty]{\mathbb{P}} 0. \quad \blacksquare$$

Next, we show that as long as the probabilistic classifier is consistent and the critical values are well estimated (which holds for large B' according to Theorem 5), the power of the ACORE test converges to the power of the LRT as B grows.

Theorem 6 For each $C \in \mathbb{R}$, let $\widehat{\phi}_{B,C}(\mathcal{D})$ be the test based on the *ACORE* statistic $\widehat{\Lambda}_B$ for a labeled sample size B with critical value C .⁴ Moreover, let $\phi_C(\mathcal{D})$ be the likelihood ratio test with critical value C . If, for every $\theta \in \Theta$, the probabilistic classifier is such that

$$\widehat{\mathbb{P}}(Y = 1|\theta, \mathbf{X}) \xrightarrow[B \rightarrow \infty]{\mathbb{P}} \mathbb{P}(Y = 1|\theta, \mathbf{X}),$$

where $|\Theta| < \infty$, and \widehat{C}_B is chosen such that $\widehat{C}_B \xrightarrow[B \rightarrow \infty]{\text{Dist}} C$ for a given $C \in \mathbb{R}$, then, for every $\theta \in \Theta$,

$$\mathbb{P}_{\mathcal{D}, \mathcal{T}|\theta} \left(\widehat{\phi}_{B, \widehat{C}_B}(\mathcal{D}) = 1 \right) \xrightarrow[B \rightarrow \infty]{} \mathbb{P}_{\mathcal{D}|\theta} (\phi_C(\mathcal{D}) = 1).$$

Proof Because $\widehat{\mathbb{P}}(Y = 1|\theta, \mathbf{X}) \xrightarrow[B \rightarrow \infty]{\mathbb{P}} \mathbb{P}(Y = 1|\theta, \mathbf{X})$, it follows directly from the properties of convergence in probability that for every $\theta_0, \theta_1 \in \Theta$

$$\sum_{i=1}^n \log \left(\widehat{\mathbb{O}\mathbb{R}}(\mathbf{X}_i^{\text{obs}}; \theta_0, \theta_1) \right) \xrightarrow[B \rightarrow \infty]{\mathbb{P}} \sum_{i=1}^n \log \left(\mathbb{O}\mathbb{R}(\mathbf{X}_i^{\text{obs}}; \theta_0, \theta_1) \right).$$

The continuous mapping theorem implies that

$$\widehat{\Lambda}_B(\mathcal{D}; \Theta_0) \xrightarrow[B \rightarrow \infty]{\mathbb{P}} \sup_{\theta_0 \in \Theta_0} \inf_{\theta_1 \in \Theta} \sum_{i=1}^n \log \left(\mathbb{O}\mathbb{R}(\mathbf{X}_i^{\text{obs}}; \theta_0, \theta_1) \right),$$

and therefore $\widehat{\Lambda}_B(\mathcal{D}; \Theta_0)$ converges in distribution to $\sup_{\theta_0 \in \Theta_0} \inf_{\theta_1 \in \Theta} \sum_{i=1}^n \log \left(\mathbb{O}\mathbb{R}(\mathbf{X}_i^{\text{obs}}; \theta_0, \theta_1) \right)$. Now, from Slutsky's theorem,

$$\begin{aligned} & \widehat{\Lambda}_B(\mathcal{D}; \Theta_0) - \widehat{C}_B \\ & \xrightarrow[B \rightarrow \infty]{\text{Dist}} \sup_{\theta_0 \in \Theta_0} \inf_{\theta_1 \in \Theta} \sum_{i=1}^n \log \left(\mathbb{O}\mathbb{R}(\mathbf{X}_i^{\text{obs}}; \theta_0, \theta_1) \right) - C. \end{aligned}$$

It follows that

$$\begin{aligned} \mathbb{P}_{\mathcal{D}, \mathcal{T}|\theta} \left(\widehat{\phi}_{B, \widehat{C}_B}(\mathcal{D}) = 1 \right) &= \mathbb{P}_{\mathcal{D}, \mathcal{T}|\theta} \left(\widehat{\Lambda}_B(\mathcal{D}; \Theta_0) - \widehat{C}_B \leq 0 \right) \\ &\xrightarrow[B \rightarrow \infty]{} \mathbb{P}_{\mathcal{D}|\theta} \left(\sup_{\theta_0 \in \Theta_0} \inf_{\theta_1 \in \Theta} \sum_{i=1}^n \log \left(\mathbb{O}\mathbb{R}(\mathbf{X}_i^{\text{obs}}; \theta_0, \theta_1) \right) - C \leq 0 \right) \\ &= \mathbb{P}_{\mathcal{D}|\theta} (\phi_C(\mathcal{D}) = 1), \end{aligned}$$

where the last equality follows from Proposition 1. ■

4. That is, $\widehat{\phi}_{B,C}(\mathcal{D}) = 1 \iff \widehat{\Lambda}_B(\mathcal{D}; \Theta_0) < C$.

Appendix E. Proofs

Proof [Proof of Proposition 1] By Bayes rule,

$$\mathbb{O}(\mathbf{x}; \theta) := \frac{\mathbb{P}(Y = 1 | \theta, \mathbf{x})}{\mathbb{P}(Y = 0 | \theta, \mathbf{x})} = \frac{f(\mathbf{x} | \theta) p}{g(\mathbf{x})(1 - p)}.$$

If $\widehat{\mathbb{P}}(Y = 1 | \theta, \mathbf{x}) = \mathbb{P}(Y = 1 | \theta, \mathbf{x})$, then $\widehat{\mathbb{O}}(\mathbf{x}; \theta_0) = \mathbb{O}(\mathbf{x}; \theta_0)$. Therefore,

$$\begin{aligned} \widehat{\tau}(\mathcal{D}; \Theta_0) &:= \frac{\int_{\Theta_0} \prod_{i=1}^n \widehat{\mathbb{O}}(\mathbf{X}_i^{\text{obs}}; \theta) d\pi_0(\theta)}{\int_{\Theta_1} \prod_{i=1}^n \widehat{\mathbb{O}}(\mathbf{X}_i^{\text{obs}}; \theta) d\pi_1(\theta)} \\ &= \frac{\int_{\Theta_0} \prod_{i=1}^n \frac{f(\mathbf{X}_i^{\text{obs}} | \theta)}{g(\mathbf{X}_i^{\text{obs}})} d\pi_0(\theta)}{\int_{\Theta_1} \prod_{i=1}^n \frac{f(\mathbf{X}_i^{\text{obs}} | \theta)}{g(\mathbf{X}_i^{\text{obs}})} d\pi_1(\theta)} \\ &= \frac{\int_{\Theta_0} \prod_{i=1}^n f(\mathbf{X}_i^{\text{obs}} | \theta) d\pi_0(\theta)}{\int_{\Theta_1} \prod_{i=1}^n f(\mathbf{X}_i^{\text{obs}} | \theta) d\pi_1(\theta)} \\ &= \frac{\int_{\Theta_0} \mathcal{L}(\mathcal{D}; \theta) d\pi_0(\theta)}{\int_{\Theta_1} \mathcal{L}(\mathcal{D}; \theta) \pi_1(\theta) d\theta} \\ &= \text{BF}(\mathcal{D}; \theta_0). \end{aligned}$$

■

Proof [Proof of Theorem 1] Assumption 1 implies that, for every D ,

$$\begin{aligned} 0 \leq |\widehat{p}(D; \Theta_0) - p(D; \Theta_0)| &= \left| \sup_{\theta \in \Theta_0} \widehat{p}(D; \theta) - \sup_{\theta \in \Theta_0} p(D; \theta) \right| \\ &\leq \sup_{\theta \in \Theta_0} |\widehat{p}(D; \theta) - p(D; \theta)| \xrightarrow[B' \rightarrow \infty]{\text{a.s.}} 0, \end{aligned}$$

and therefore $\widehat{p}(D; \Theta_0)$ converges almost surely to $p(D; \Theta_0)$. It follows that $\widehat{p}(\mathcal{D}; \Theta_0)$ converges in distribution to $p(\mathcal{D}; \Theta_0)$. Conclude that

$$\mathbb{P}_{\mathcal{D}, \mathcal{T}' | \theta}(\widehat{p}(\mathcal{D}; \Theta_0) \leq \alpha) = F_{\widehat{p}(\mathcal{D}; \Theta_0) | \theta}(\alpha) \xrightarrow[B' \rightarrow \infty]{} F_{p(\mathcal{D}; \Theta_0) | \theta}(\alpha) = \mathbb{P}_{\mathcal{D} | \theta}(p(\mathcal{D}; \Theta_0) \leq \alpha),$$

where F_Z denotes the cumulative distribution function of the random variable Z . ■

Proof [Proof of Corollary 1] Fix $\theta \in \Theta$. Because F_θ is continuous, the definition of $p(\mathcal{D}; \theta)$ implies that its distribution is uniform under the null. Thus $\mathbb{P}_{\mathcal{D} | \theta}(p(\mathcal{D}; \theta) \leq \alpha) = \alpha$. Theorem 1 therefore implies that

$$\mathbb{P}_{\mathcal{D}, \mathcal{T}' | \theta}(\widehat{p}(\mathcal{D}; \theta) \leq \alpha) \xrightarrow[B' \rightarrow \infty]{} \mathbb{P}_{\mathcal{D} | \theta}(p(\mathcal{D}; \theta) \leq \alpha) = \alpha. \quad (19)$$

Now, for any $\theta \in \Theta_0$, uniformity of the p-value implies that

$$\begin{aligned} \mathbb{P}_{\mathcal{D} | \theta}(p(\mathcal{D}; \Theta_0) \leq \alpha) &= \mathbb{P}_{\mathcal{D} | \theta} \left(\sup_{\theta_0 \in \Theta_0} p(\mathcal{D}; \theta_0) \leq \alpha \right) \leq \mathbb{P}_{\mathcal{D} | \theta}(p(\mathcal{D}; \theta) \leq \alpha) \\ &= \alpha. \end{aligned}$$

Conclude from Theorem 1 that

$$\mathbb{P}_{\mathcal{D}, \mathcal{T}'|\theta}(\widehat{p}(\mathcal{D}; \Theta_0) \leq \alpha) \xrightarrow{B' \rightarrow \infty} \mathbb{P}_{\mathcal{D}|\theta}(p(\mathcal{D}; \Theta_0) \leq \alpha) \leq \alpha. \quad (20)$$

The conclusion follows from putting together Equations 19 and 20. \blacksquare

Proof [Proof of Theorem 2]

$$\begin{aligned} |\widehat{p}(D; \Theta_0) - p(D; \Theta_0)| &= \left| \sup_{\theta \in \Theta_0} \widehat{p}(D; \theta) - \sup_{\theta \in \Theta_0} p(D; \theta) \right| \\ &\leq \sup_{\theta \in \Theta_0} |\widehat{p}(D; \theta) - p(D; \theta)| \\ &= O_P \left(\left(\frac{1}{B'} \right)^r \right), \end{aligned}$$

where the last line follows from Assumption 2 \blacksquare

Lemma 1 Under Assumption 4, $\int (\mathbb{O}(\mathbf{x}; \theta_0) - \widehat{\mathbb{O}}(\mathbf{x}; \theta_0))^2 dG(\mathbf{x}) \leq \frac{M'}{m'} L(\widehat{\mathbb{O}}, \mathbb{O})$.

Proof Let h be as in Assumption 4. Notice that

$$\begin{aligned} \int (\mathbb{O}(\mathbf{x}; \theta_0) - \widehat{\mathbb{O}}(\mathbf{x}; \theta_0))^2 dG(\mathbf{x}) &\leq \sup_{\theta \in \Theta} \int (\mathbb{O}(\mathbf{x}; \theta) - \widehat{\mathbb{O}}(\mathbf{x}; \theta))^2 dG(\mathbf{x}) \\ &\leq M' \leq \frac{M'}{m'} \int h(\theta) d\pi(\theta) \\ &= \frac{M'}{m'} L(\widehat{\mathbb{O}}, \mathbb{O}), \end{aligned}$$

which concludes the proof. \blacksquare

Lemma 2 Under Assumptions 3 and 4, there exists $K > 0$ such that

$$\mathbb{E}_{\mathcal{D}|\theta, T} [|\tau(\mathcal{D}; \theta_0) - \widehat{\tau}_B(\mathcal{D}; \theta_0)|] \leq K \sqrt{L(\widehat{\mathbb{O}}, \mathbb{O})}.$$

Proof For every $\theta \in \Theta$

$$\begin{aligned} \mathbb{E}_{\mathcal{D}|\theta, T}^2 [|\tau(\mathcal{D}; \theta_0) - \widehat{\tau}_B(\mathcal{D}; \theta_0)|] &= \left(\int |\tau(\mathcal{D}; \theta_0) - \widehat{\tau}_B(\mathcal{D}; \theta_0)| dF(\mathbf{x}|\theta) \right)^2 \\ &= \left(\int |\mathbb{O}(\mathbf{x}; \theta_0) - \widehat{\mathbb{O}}(\mathbf{x}; \theta_0)| dF(\mathbf{x}|\theta) \right)^2 \\ &= \left(\int |\mathbb{O}(\mathbf{x}; \theta_0) - \widehat{\mathbb{O}}(\mathbf{x}; \theta_0)| \mathbb{O}(\mathbf{x}; \theta) dG(\mathbf{x}) \right)^2 \\ &\leq \left(\int (\mathbb{O}(\mathbf{x}; \theta_0) - \widehat{\mathbb{O}}(\mathbf{x}; \theta_0))^2 dG(\mathbf{x}) \right) \left(\int \mathbb{O}^2(\mathbf{x}; \theta) dG(\mathbf{x}) \right), \end{aligned}$$

where the last inequality follows from Cauchy-Schwarz. Assumption 3 implies that

$$\int \mathbb{O}^2(\mathbf{x}; \theta) dG(\mathbf{x}) \leq M^2,$$

from which we conclude that

$$\mathbb{E}_{\mathcal{D}|\theta, T}^2 [|\tau(\mathcal{D}; \theta_0) - \hat{\tau}_B(\mathcal{D}; \theta_0)|] \leq M^2 \int (\mathbb{O}(\mathbf{x}; \theta_0) - \hat{\mathbb{O}}(\mathbf{x}; \theta_0))^2 dG(\mathbf{x}).$$

Conclude from Lemma 1 that

$$\mathbb{E}_{\mathcal{D}|\theta, T}^2 [|\tau(\mathcal{D}; \theta_0) - \hat{\tau}_B(\mathcal{D}; \theta_0)|] \leq K^2 \cdot L(\hat{\mathbb{O}}, \mathbb{O}),$$

where $K = M\sqrt{\frac{M'}{m'}}$. ■

Lemma 3 *Under Assumptions 3-7, there exists $C > 0$ such that*

$$\mathbb{E}_{\mathcal{D}, T|\theta} [|\tau(\mathcal{D}; \theta_0) - \hat{\tau}_B(\mathcal{D}; \theta_0)|] \leq CB^{-\kappa/(2(\kappa+d))}.$$

Proof Let $\hat{p} = \hat{\mathbb{P}}(Y = 1|\mathbf{x}, \theta)$ and $p = \mathbb{P}(Y = 1|\mathbf{x}, \theta)$ be the probabilistic classifier and true classification function, respectively, on the training sample T . Let $h(y) = \frac{y}{1-y}$ for $0 < y < 1$. A Taylor expansion of h implies that

$$(h(\hat{p}) - h(p))^2 = (h(p) + R_1(\hat{p}) - h(p))^2 = R_1(\hat{p})^2,$$

where $R_1(\hat{p}) = h'(\xi)(\hat{p} - p)$ for some ξ between p and \hat{p} . Also note that due to Assumption 3,

$$\exists a > 0 \text{ s.t. } p, \hat{p} > a, \forall x \in \mathcal{X}, \theta \in \Theta.$$

Thus,

$$\begin{aligned} \mathbb{E}_{\mathcal{T}} \left[\int (h(\hat{p}) - h(p))^2 dG(\mathbf{x}) d\pi(\theta) \right] &= \mathbb{E}_{\mathcal{T}} \left[\int \frac{1}{(1-\xi)^4} (\hat{p} - p)^2 dG(\mathbf{x}) d\pi(\theta) \right] \\ &\leq \frac{1}{(1-a)^4} \mathbb{E}_{\mathcal{T}} \left[\int (\hat{p} - p)^2 dG(\mathbf{x}) d\pi(\theta) \right] \\ &= \frac{1}{(1-a)^4} \mathbb{E}_{\mathcal{T}} \left[\int \left(\hat{\mathbb{P}}(Y = 1|\mathbf{x}, \theta) - \mathbb{P}(Y = 1|\mathbf{x}, \theta) \right)^2 h'(\mathbf{x}, \theta) dH(\mathbf{x}, \theta) \right] \\ &\leq \frac{\gamma}{(1-a)^4} \mathbb{E}_{\mathcal{T}} \left[\int \left(\hat{\mathbb{P}}(Y = 1|\mathbf{x}, \theta) - \mathbb{P}(Y = 1|\mathbf{x}, \theta) \right)^2 dH(\mathbf{x}, \theta) \right] \\ &= O\left(B^{-\kappa/(\kappa+d)}\right) \end{aligned}$$

It follows that

$$\begin{aligned}
\mathbb{E}_{\mathcal{D}, \mathcal{T}|\theta} [|\tau(\mathcal{D}; \theta_0) - \hat{\tau}_B(\mathcal{D}; \theta_0)|] &= \mathbb{E}_{\mathcal{T}} [\mathbb{E}_{\mathcal{D}|\theta, \mathcal{T}} [|\tau(\mathcal{D}; \theta_0) - \hat{\tau}_B(\mathcal{D}; \theta_0)|]] \\
&\leq \mathbb{E}_{\mathcal{T}} \left[K \sqrt{L(\hat{\mathbb{O}}, \mathbb{O})} \right] \\
&\leq K \sqrt{\mathbb{E}_{\mathcal{T}} [L(\hat{\mathbb{O}}, \mathbb{O})]} \\
&= K \sqrt{\mathbb{E}_{\mathcal{T}} \left[\int (h(\hat{p}) - h(p))^2 dG(\mathbf{x}) d\pi(\theta) \right]} \\
&= O \left(B^{-\kappa/(2(\kappa+d))} \right),
\end{aligned}$$

where the second inequality follows from Lemma 2. \blacksquare

Proof [Proof of Theorem 3] It follows from Markov's inequality that with probability at least $1 - \epsilon$, \mathcal{D} is such that

$$|\tau(\mathcal{D}; \theta_0) - \hat{\tau}(\mathcal{D}; \theta_0)| \leq \frac{K \cdot \sqrt{L(\hat{\mathbb{O}}, \mathbb{O})}}{\epsilon} \quad (21)$$

Now we upper bound $\mathbb{P}_{\theta}(\phi_{\tau}(\mathcal{D}) \neq \phi_{\hat{\tau}}(\mathcal{D}))$. Define A as the event that Eq. 21 happens. Then:

$$\begin{aligned}
\mathbb{P}_{\mathcal{D}|\theta, T}(\phi_{\tau}(\mathcal{D}) \neq \phi_{\hat{\tau}}(\mathcal{D})) &\leq \mathbb{P}_{\mathcal{D}|\theta, T}(\phi_{\tau}(\mathcal{D}) \neq \phi_{\hat{\tau}}(\mathcal{D}), A) + \mathbb{P}_{\theta}(A^c) \\
&\leq \mathbb{P}_{\mathcal{D}|\theta, T}(\mathbb{I}(\tau(\mathcal{D}; \theta_0) < c) \neq \mathbb{I}(\hat{\tau}(\mathcal{D}; \theta_0) < c), A) + \epsilon \\
&\leq \mathbb{P}_{\mathcal{D}|\theta, T} \left(c - \frac{K \cdot \sqrt{L(\hat{\mathbb{O}}, \mathbb{O})}}{\epsilon} < \tau(\mathcal{D}; \theta_0) < c + \frac{K \cdot \sqrt{L(\hat{\mathbb{O}}, \mathbb{O})}}{\epsilon} \right) + \epsilon
\end{aligned}$$

Assumption 5 then implies that

$$\mathbb{P}_{\mathcal{D}|\theta, T}(\phi_{\tau}(\mathcal{D}) \neq \phi_{\hat{\tau}}(\mathcal{D})) \leq \frac{K' \cdot \sqrt{L(\hat{\mathbb{O}}, \mathbb{O})}}{\epsilon} + \epsilon$$

where $K' = 2KC_L$, which concludes the proof. \blacksquare

Proof [Proof of Theorem 4] It follows from Markov's inequality that with probability at least $1 - \epsilon$, \mathcal{D} is such that

$$|\tau(\mathcal{D}; \theta_0) - \hat{\tau}(\mathcal{D}; \theta_0)| \leq \frac{CB^{-\kappa/(2(\kappa+d))}}{\epsilon} \quad (22)$$

Following the same reasoning as for Theorem 3, we obtain that

$$\mathbb{P}_{\mathcal{D}, \mathcal{T}|\theta}(\phi_{\tau}(\mathcal{D}) \neq \phi_{\hat{\tau}}(\mathcal{D})) \leq \frac{K'' B^{-\kappa/(2(\kappa+d))}}{\epsilon} + \epsilon$$

where $K'' = 2CC_L$. Notice that taking $\epsilon^* = \sqrt{K''}B^{-\kappa/(4(\kappa+d))}$ optimizes the bound and gives the result. \blacksquare

Proof [Proof of Corollary 2] The result follows from noticing that

$$\begin{aligned} \mathbb{P}_{\mathcal{D}, \mathcal{T}|\theta}(\phi_{\hat{\tau}_B}(\mathcal{D}) = 1) &\geq \mathbb{P}_{\mathcal{D}, \mathcal{T}|\theta}(\phi_{\tau}(\mathcal{D}) = 1) - \mathbb{P}_{\mathcal{D}, \mathcal{T}|\theta}(\phi_{\tau}(\mathcal{D}) \neq \phi_{\hat{\tau}_B}(\mathcal{D})) \\ &\geq \mathbb{P}_{\mathcal{D}, \mathcal{T}|\theta}(\phi_{\tau}(\mathcal{D}) = 1) - 2\sqrt{K''}B^{-\kappa/(4(\kappa+d))}, \end{aligned}$$

where the last inequality follows from Theorem 4. \blacksquare

Appendix F. Multivariate Gaussian Example

In this section, we include (i) the analytical derivations for the marginal distribution and Bayes factor in the multivariate Gaussian setting, and (ii) Section 7.2.2 details for the probabilistic classifier selection and the analysis of the drop in power for ACORE and BFF at $d = 5$ and $d = 10$.

F.1 Analytical Derivations

Given that the covariance matrix is $\Sigma = I_d$ in this setting, the marginal distribution $F_{\mathbf{X}}$ has a closed form solution for any $\mathbf{a}, \mathbf{b} \in \mathbb{R}^d$, which can be expressed as follows:

$$\begin{aligned} F_{\mathbf{X}}(\mathbf{x}) &= \int_{\mathbf{a}}^{\mathbf{b}} (2\pi)^{-\frac{d}{2}} \det(\Sigma)^{-\frac{1}{2}} \exp\left(-\frac{1}{2}(\mathbf{x} - \boldsymbol{\mu})^T \Sigma^{-1}(\mathbf{x} - \boldsymbol{\mu})\right) d\boldsymbol{\mu} \\ &= \int_{\mathbf{a}}^{\mathbf{b}} (2\pi)^{-\frac{d}{2}} \exp\left(-\frac{1}{2}\left(\sum_{i=1}^d x_i^2 - 2x_i\mu_i + \mu_i^2\right)\right) d\mu_1 d\mu_2 \dots d\mu_d \\ &= \prod_{i=1}^d \left[\int_{a_i}^{b_i} (2\pi)^{-\frac{1}{2}} \exp\left(-\frac{1}{2}x_i^2 + x_i\mu_i - \frac{1}{2}\mu_i^2\right) d\mu_i \right] \\ &= \prod_{i=1}^d \frac{1}{2} \operatorname{erf}\left(\frac{b_i - x_i}{\sqrt{2}}\right) - \frac{1}{2} \operatorname{erf}\left(\frac{a_i - x_i}{\sqrt{2}}\right), \end{aligned}$$

In this setting, the proposal distribution π is uniform over an axis-aligned hyper-rectangle with extremes $\mathbf{a} = (a, \dots, a)$ and $\mathbf{b} = (b, \dots, b)$ for $a < b \in \mathbb{R}$. Since $\bar{\mathbf{X}}_n$ is a sufficient statistic, the exact Bayes factor for the Neyman construction when testing $H_{0, \theta_0} : \theta = \theta_0$ versus $H_{1, \theta_0} : \theta \neq \theta_0$ is equal to:

$$\begin{aligned}
\text{BF}(\mathcal{D}; \theta_0) &= \frac{N(\bar{\mathbf{X}}_n; \theta_0, n^{-1}I_d)}{\int_{\mathbf{a}}^{\mathbf{b}} N(\bar{\mathbf{X}}_n; \theta, n^{-1}I_d) d\pi(\theta)} \\
&= \frac{N(\bar{\mathbf{X}}_n; \theta_0, n^{-1}I_d)}{\left(\frac{1}{b-a}\right)^d \int_{\mathbf{a}}^{\mathbf{b}} N(\bar{\mathbf{X}}_n; \theta, n^{-1}I_d) d\theta} \\
&= \frac{N(\bar{\mathbf{X}}_n; \theta_0, n^{-1}I_d)}{\left(\frac{1}{b-a}\right)^d \prod_{j=1}^d \left[\frac{1}{2} \text{erf}\left(\frac{b-\bar{X}_{n,j}}{\sqrt{2n}}\right) - \frac{1}{2} \text{erf}\left(\frac{a-\bar{X}_{n,j}}{\sqrt{2n}}\right) \right]},
\end{aligned}$$

where $\bar{X}_{n,j}$ is the j -th coordinate of $\bar{\mathbf{X}}_n$.

F.2 Section 7.2.2 Details

Figure 10 (left) compares cross-entropy loss curves for the QDA (the best classifier for the Gaussian likelihood model) and MLP classifiers. As we increase B , odds estimation becomes more accurate, and we expect to see a decrease in both cross-entropy loss and integrated odds loss, as shown in Figure 10 (right).

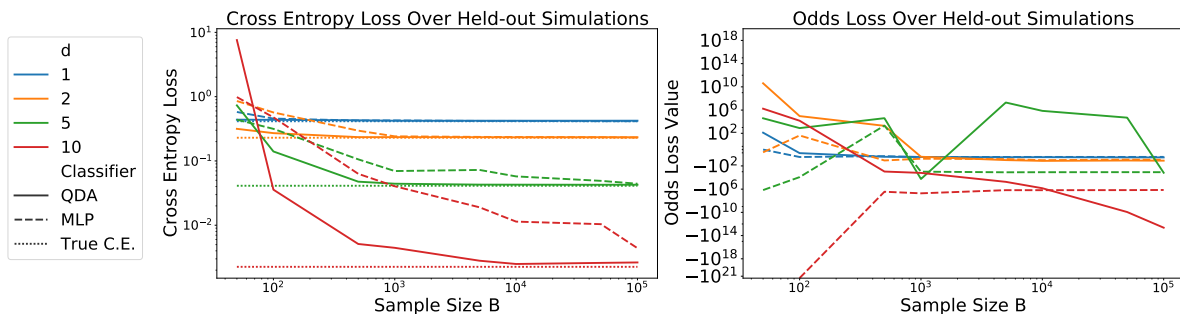


Figure 10: *Left*: Cross-entropy loss in learning the odds versus the sample size B (Algorithm 3) for a QDA and MLP classifier, as well as the true cross entropy, for the Gaussian likelihood model in dimensions $d = 1, 2, 5$ and 10 . QDA has the lowest cross-entropy loss among the classifiers we considered (of which MLP is one example). The values B at which the cross entropy plateaus are used as the sample sizes for learning the odds at various dimensions. *Right*: The integrated odds loss generally decreases with increasing B , as expected, though it is noisier (the presence of small probabilities blows up the odds ratio). For larger values of B , the integrated odds loss should be more stable.

We showed in Section 4 that the power of BFF is bounded by the integrated odds loss. In practice, this loss may be more stably estimated for larger B , which would make it an attractive alternative to the cross-entropy loss. The performance difference in Figure 10 is reflected in Figure 11, highlighting the importance of choosing the best fitting classifier.

To pinpoint the cause of the degradation in power in high dimensions for ACORE and BFF in Section 7.2.2, we separate the error in estimating the odds from the numerical error

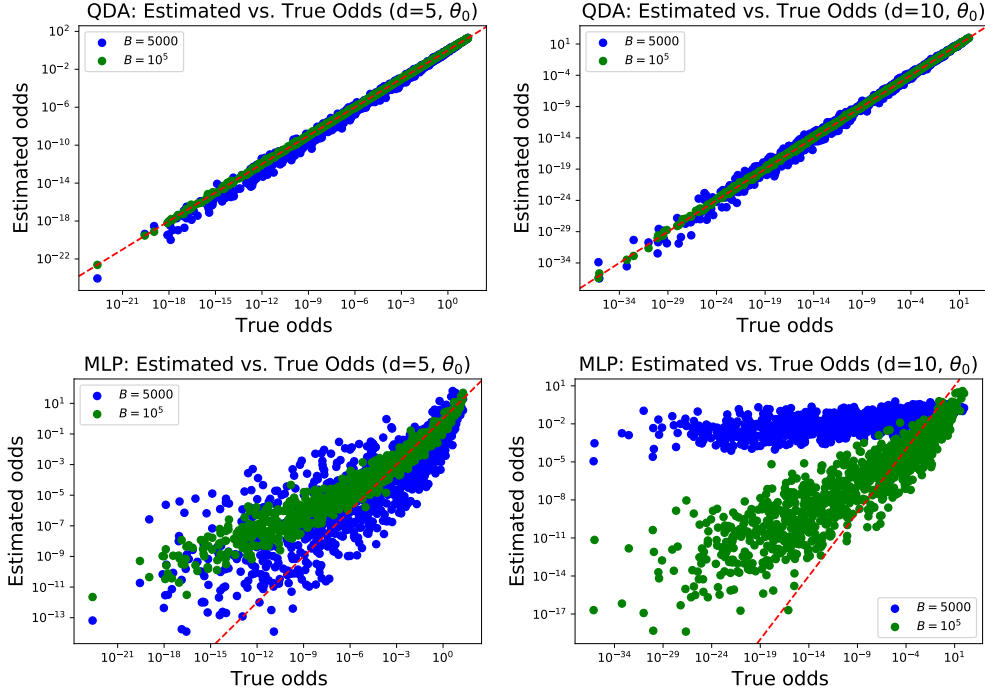


Figure 11: Odds classifiers trained on B samples, evaluated on 1000 test samples. QDA (top row) fits better than MLP (bottom row), and QDA with $B = 10^5$ fits well.

in the maximization or integration step for the test statistic (errors e_1 and e_2 in Section 5). Figure 11 shows that the QDA estimation error is negligible at both $d = 5$ and $d = 10$ (as opposed to MLP estimation error). To isolate the numerical error, Figure 12 shows the estimated ACORE and BFF statistics using the analytical odds function. Even with a large budget of $M = 30000$, we underestimate both the odds maximum and the integrated odds across the parameter space, resulting in an over-estimation of the ACORE and BFF test statistics.

Appendix G. Computational Stability for BFF

When computing the BFF statistics for the Neyman construction hypothesis testing, the denominator is approximated by an average in the following way:

$$\tau(\mathcal{D}; \theta_0) := \frac{\prod_{i=1}^n \mathbb{O}(\mathbf{X}_i; \theta_0)}{\int_{\Theta} (\prod_{i=1}^n \mathbb{O}(\mathbf{X}_i; \theta)) d\pi(\theta)} \approx \frac{\prod_{i=1}^n \mathbb{O}(\mathbf{X}_i; \theta_0)}{\frac{1}{m} \sum_{j=1}^m \prod_{i=1}^n \mathbb{O}(\mathbf{X}_i; \theta_j)},$$

where $\theta_j \sim \pi(\theta)$ for $j = 1, \dots, m$. In practice, the product of odds can quickly run into overflow/underflow. If one assumes $m \leq \mathbb{O}(\mathbf{X}_i; \theta_j) \leq M$ for all \mathbf{X}_i, θ_j , the product over n samples can range from $m^n \leq \prod_{i=1}^n \mathbb{O}(\mathbf{X}_i; \theta_j) \leq M^n$ which could be below or above machine precision depending on the values of m and M respectively. Running computations in log-

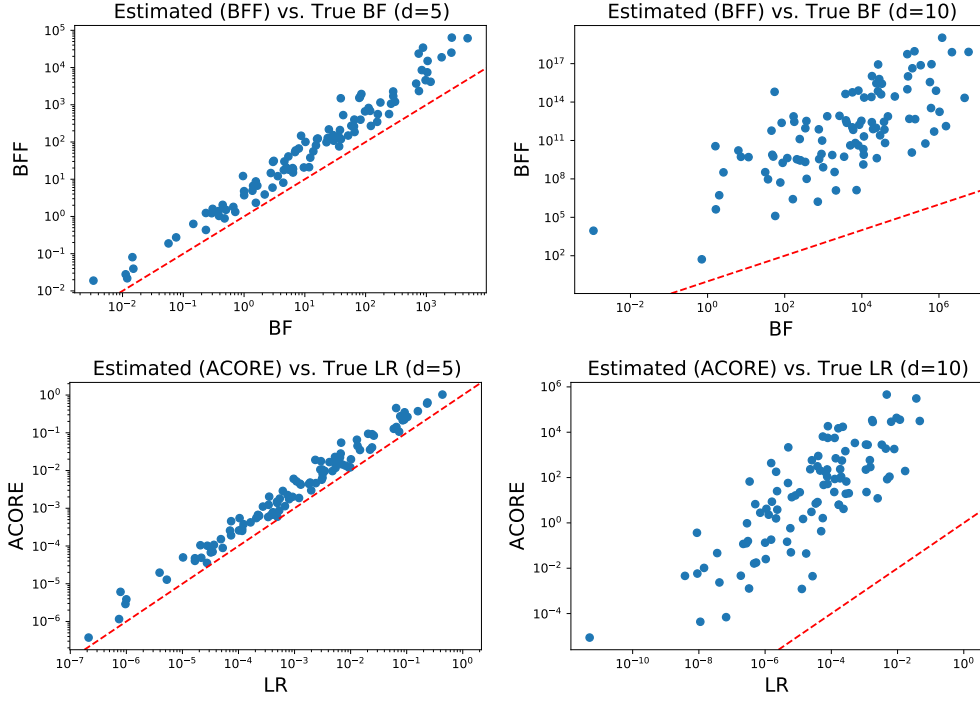


Figure 12: We estimate the BFF and ACORE test statistics using exact odds, so the only error is due to numerical estimation of the denominator with $N = 30000$ uniform samples. We see that as d grows, this numerical estimation quickly becomes imprecise, even for large values of N .

space provides computationally stable calculations even for large samples. First, we can express the test statistic approximation in the following way:

$$\tau(\mathcal{D}; \theta_0) \approx \frac{\prod_{i=1}^n \mathbb{O}(\mathbf{X}_i; \theta_0)}{\frac{1}{m} \sum_{j=1}^m \prod_{i=1}^n \mathbb{O}(\mathbf{X}_i; \theta_j)} = \frac{\exp \sum_{i=1}^n \log(\mathbb{O}(\mathbf{X}_i; \theta_0))}{\frac{1}{m} \sum_{j=1}^m \exp \sum_{i=1}^n \log(\mathbb{O}(\mathbf{X}_i; \theta_j))}.$$

Let $\psi^0 = \sum_{i=1}^n \log(\mathbb{O}(\mathbf{X}_i; \theta_0))$ and $\psi_j = \sum_{i=1}^n \log(\mathbb{O}(\mathbf{X}_i; \theta_j))$. Computing the log-space version of the BFF test statistics then leads to

$$\log(\tau(\mathcal{D}; \theta_0)) = \psi^0 - \log \left(\frac{1}{m} \sum_{j=1}^m \exp^{\psi_j} \right) = \psi^0 + \log(m) - \log \left(\sum_{j=1}^m \exp^{\psi_j} \right).$$

The above can be made computationally stable by using any of the “log-sum-exp” implementations available (such as in SciPy, Virtanen et al. (2020)).

References

- G. Aad, T. Abajyan, B. Abbott, J. Abdallah, S. Abdel Khalek, A. Abdelalim, O. Abdinov, R. Aben, B. Abi, M. Abolins, et al. Observation of a new particle in the search for the Standard Model Higgs boson with the ATLAS detector at the LHC. *Physics Letters B*, 716(1):1–29, Sep 2012. ISSN 0370-2693. doi: 10.1016/j.physletb.2012.08.020.
- T. Ayano. Rates of convergence for the k-nearest neighbor estimators with smoother regression functions. *Journal of Statistical Planning and Inference*, 142(9):2530–2536, 2012.
- M. A. Beaumont, W. Zhang, and D. J. Balding. Approximate Bayesian computation in population genetics. *Genetics*, 162(4):2025–2035, 2002.
- J. Bendavid. Efficient Monte Carlo integration using boosted decision trees and generative deep neural networks. *arXiv preprint arXiv:1707.00028*, 6 2017.
- G. Biau. Analysis of a random forests model. *The Journal of Machine Learning Research*, 13(1):1063–1095, 2012.
- P. J. Bickel and B. Li. Local polynomial regression on unknown manifolds. *Complex datasets and inverse problems*, pages 177–186, 2007.
- H. J. Bierens. Uniform consistency of kernel estimators of a regression function under generalized conditions. *Journal of the American Statistical Association*, 78(383):699–707, 1983.
- R. Bordoloi, S. J. Lilly, and A. Amara. Photo-z performance for precision cosmology. *Monthly Notices of the Royal Astronomical Society*, 406(2):881–895, 2010.
- J. Brehmer, K. Cranmer, G. Louppe, and J. Pavez. Constraining effective field theories with machine learning. *Physical Review Letters*, 121(11), Sep 2018. ISSN 1079-7114. doi: 10.1103/physrevlett.121.111801.
- J. Brehmer, F. Kling, I. Espejo, and K. Cranmer. Madminer: Machine learning-based inference for particle physics. *Computing and Software for Big Science*, 4(1):1–25, 2020a.
- J. Brehmer, G. Louppe, J. Pavez, and K. Cranmer. Mining gold from implicit models to improve likelihood-free inference. *Proceedings of the National Academy of Sciences*, 117(10):5242–5249, 2020b. ISSN 0027-8424. doi: 10.1073/pnas.1915980117.
- J. Chen and P. Li. Hypothesis test for normal mixture models: The EM approach. *The Annals of Statistics*, 37(5A):2523–2542, 2009.
- Y. Chen and M. U. Gutmann. Adaptive Gaussian copula ABC. In K. Chaudhuri and M. Sugiyama, editors, *Proceedings of Machine Learning Research*, volume 89 of *Proceedings of Machine Learning Research*, pages 1584–1592. PMLR, 16–18 Apr 2019.
- C.-S. Chuang and T. L. Lai. Hybrid resampling methods for confidence intervals. *Statistica Sinica*, 10(1):1–33, 2000. ISSN 10170405, 19968507.

- S. R. Cook, A. Gelman, and D. B. Rubin. Validation of software for Bayesian models using posterior quantiles. *Journal of Computational and Graphical Statistics*, 15(3):675–692, 2006. doi: 10.1198/106186006X136976.
- R. D. Cousins. Lectures on statistics in theory: Prelude to statistics in practice, 2018.
- G. Cowan. Discovery sensitivity for a counting experiment with background uncertainty. *Technical Report*, 2012.
- G. Cowan, K. Cranmer, E. Gross, and O. Vitells. Asymptotic formulae for likelihood-based tests of new physics. *The European Physical Journal C*, 71(2), Feb 2011. ISSN 1434-6052. doi: 10.1140/epjc/s10052-011-1554-0.
- K. Cranmer. Practical Statistics for the LHC. *arXiv e-prints*, art. arXiv:1503.07622, Mar 2015.
- K. Cranmer, J. Pavez, and G. Louppe. Approximating likelihood ratios with calibrated discriminative classifiers. *arXiv preprint arXiv:1506.02169*, 2015.
- K. Cranmer, J. Brehmer, and G. Louppe. The frontier of simulation-based inference. *Proceedings of the National Academy of Sciences*, 117(48):30055–30062, 2020. ISSN 0027-8424. doi: 10.1073/pnas.1912789117.
- D. Dacunha-Castelle and E. Gassiat. Testing in locally conic models, and application to mixture models. *ESAIM: Probability and Statistics*, 1:285–317, 1997.
- N. Dalmaso, R. Izbicki, and A. Lee. Confidence sets and hypothesis testing in a likelihood-free inference setting. In H. D. III and A. Singh, editors, *Proceedings of the 37th International Conference on Machine Learning*, volume 119 of *Proceedings of Machine Learning Research*, pages 2323–2334, Virtual, 13–18 Jul 2020. PMLR.
- L. Devroye, L. Györfi, and G. Lugosi. *A Probabilistic Theory of Pattern Recognition*, volume 31. Springer Science & Business Media, 2013.
- D. L. Donoho. Asymptotic minimax risk for sup-norm loss: solution via optimal recovery. *Probability Theory and Related Fields*, 99(2):145–170, 1994.
- M. Drton. Likelihood ratio tests and singularities. *The Annals of Statistics*, 37(2):979–1012, Apr 2009. ISSN 0090-5364. doi: 10.1214/07-aos571.
- C. Durkan, I. Murray, and G. Papamakarios. On contrastive learning for likelihood-free inference. In H. D. III and A. Singh, editors, *Proceedings of the 37th International Conference on Machine Learning*, volume 119 of *Proceedings of Machine Learning Research*, pages 2771–2781. PMLR, 13–18 Jul 2020.
- M. Fasiolo, S. N. Wood, F. Hartig, and M. V. Bravington. An extended empirical saddle-point approximation for intractable likelihoods. *Electron. J. Statist.*, 12(1):1544–1578, 2018. doi: 10.1214/18-EJS1433.
- G. Feldman. Multiple measurements and parameters in the unified approach. Technical report, Technical Report, Talk at the FermiLab Workshop on Confidence Limits, 2000.

- G. J. Feldman and R. D. Cousins. Unified approach to the classical statistical analysis of small signals. *Physical Review D*, 57(7):3873–3889, Apr 1998. ISSN 1089-4918. doi: 10.1103/physrevd.57.3873.
- F. Feroz, M. P. Hobson, and M. Bridges. Multinest: an efficient and robust Bayesian inference tool for cosmology and particle physics. *Monthly Notices of the Royal Astronomical Society*, 398(4):1601–1614, Oct 2009. ISSN 1365-2966. doi: 10.1111/j.1365-2966.2009.14548.x.
- M. Feurer and F. Hutter. *Hyperparameter Optimization*, pages 3–33. Springer International Publishing, Cham, 2019. ISBN 978-3-030-05318-5. doi: 10.1007/978-3-030-05318-5_1.
- R. Fisher. *Statistical Methods for Research Workers*. Oliver and Boyd: Edinburgh, 11th ed. rev. edition, 1925.
- M. Frate, K. Cranmer, S. Kalia, A. Vand enberg-Rodes, and D. Whiteson. Modeling Smooth Backgrounds and Generic Localized Signals with Gaussian Processes. *arXiv e-prints*, art. arXiv:1709.05681, Sep 2017.
- C. Gao, J. Isaacson, and C. Krause. i-flow: High-dimensional integration and sampling with normalizing flows. *Machine Learning: Science and Technology*, 1(4):045023, Nov 2020. ISSN 2632-2153. doi: 10.1088/2632-2153/abab62.
- S. Girard, A. Guillaou, and G. Stupfler. Uniform strong consistency of a frontier estimator using kernel regression on high order moments. *ESAIM: Probability and Statistics*, 18: 642–666, 2014.
- D. Greenberg, M. Nonnenmacher, and J. Macke. Automatic posterior transformation for likelihood-free inference. In K. Chaudhuri and R. Salakhutdinov, editors, *Proceedings of the 36th International Conference on Machine Learning*, volume 97 of *Proceedings of Machine Learning Research*, pages 2404–2414, Long Beach, California, USA, 09–15 Jun 2019. PMLR.
- M. U. Gutmann and J. Corander. Bayesian optimization for likelihood-free inference of simulator-based statistical models. *Journal of Machine Learning Research*, 17(125):1–47, 2016.
- L. Györfi, M. Kohler, A. Krzyzak, and H. Walk. *A Distribution-Free Theory of Nonparametric Regression*. Springer Science & Business Media, 2006.
- W. J. Handley, M. P. Hobson, and A. N. Lasenby. PolyChord: next-generation nested sampling. *Monthly Notices of the Royal Astronomical Society*, 453(4):4385–4399, Sep 2015. ISSN 1365-2966. doi: 10.1093/mnras/stv1911.
- W. Hardle, S. Luckhaus, et al. Uniform consistency of a class of regression function estimators. *The Annals of Statistics*, 12(2):612–623, 1984.
- J. Hermans, V. Begy, and G. Louppe. Likelihood-free MCMC with amortized approximate ratio estimators. *arXiv preprint arXiv:1903.04057*, 2020.

- R. Izbicki, A. Lee, and C. Schafer. High-Dimensional Density Ratio Estimation with Extensions to Approximate Likelihood Computation. In S. Kaski and J. Corander, editors, *Proceedings of the Seventeenth International Conference on Artificial Intelligence and Statistics*, volume 33 of *Proceedings of Machine Learning Research*, pages 420–429, Reykjavik, Iceland, 22–25 Apr 2014. PMLR.
- R. Izbicki, A. B. Lee, and T. Pospisil. ABC–CDE: Toward Approximate Bayesian Computation with complex high-dimensional data and limited simulations. *Journal of Computational and Graphical Statistics*, pages 1–20, 2019. doi: 10.1080/10618600.2018.1546594.
- S. Jadach. Foam: A general-purpose cellular Monte Carlo event generator. *Computer Physics Communications*, 152(1):55 – 100, 2003. ISSN 0010-4655. doi: [https://doi.org/10.1016/S0010-4655\(02\)00755-5](https://doi.org/10.1016/S0010-4655(02)00755-5).
- H. Jeffreys. Some tests of significance, treated by the theory of probability. *Mathematical Proceedings of the Cambridge Philosophical Society*, 31(2):203–222, 1935. doi: 10.1017/S030500410001330X.
- H. Jeffreys. *Theory of probability*. Clarendon Press Oxford, 3rd ed. edition, 1961.
- M. Järvenpää, M. U. Gutmann, A. Vehtari, and P. Marttinen. Parallel Gaussian process surrogate Bayesian inference with noisy likelihood evaluations. *Bayesian Anal.*, 16(1): 147–178, 2021. doi: 10.1214/20-BA1200.
- K. Kandasamy, J. Schneider, and B. Póczos. High dimensional Bayesian optimisation and bandits via additive models. In F. Bach and D. Blei, editors, *Proceedings of the 32nd International Conference on Machine Learning*, volume 37 of *Proceedings of Machine Learning Research*, pages 295–304, Lille, France, 07–09 Jul 2015. PMLR.
- R. Koenker, V. Chernozhukov, X. He, and L. Peng. *Handbook of quantile regression*. CRC press, 2017.
- S. Kpotufe. k-NN Regression Adapts to Local Intrinsic Dimension. *Advances in Neural Information Processing Systems*, pages 729–737, 2011.
- S. Kpotufe and V. Garg. Adaptivity to local smoothness and dimension in kernel regression. *Advances in Neural Information Processing Systems*, 26:3075–3083, 2013.
- L. Li, K. Jamieson, G. DeSalvo, A. Rostamizadeh, and A. Talwalkar. Hyperband: A novel bandit-based approach to hyperparameter optimization. *Journal of Machine Learning Research*, 18-185:1–52, 2018.
- H. Liero. Strong uniform consistency of nonparametric regression function estimates. *Probability theory and related fields*, 82(4):587–614, 1989.
- J.-M. Lueckmann, P. J. Goncalves, G. Bassetto, K. Öcal, M. Nonnenmacher, and J. H. Macke. Flexible statistical inference for mechanistic models of neural dynamics. In I. Guyon, U. V. Luxburg, S. Bengio, H. Wallach, R. Fergus, S. Vishwanathan, and R. Garnett, editors, *Advances in Neural Information Processing Systems 30*, pages 1289–1299. Curran Associates, Inc., 2017.

- J.-M. Lueckmann, G. Bassetto, T. Karaletsos, and J. H. Macke. Likelihood-free inference with emulator networks. In *Symposium on Advances in Approximate Bayesian Inference*, pages 32–53, 2019.
- L. Lyons. Open statistical issues in Particle Physics. *The Annals of Applied Statistics*, 2(3):887 – 915, 2008. doi: 10.1214/08-AOAS163.
- J.-M. Marin, P. Pudlo, C. Robert, and R. Ryder. Approximate Bayesian computational methods. *Statistics and Computing*, 22:1167–1180, 11 2012. doi: 10.1007/s11222-011-9288-2.
- J.-M. Marin, L. Raynal, P. Pudlo, M. Ribatet, and C. Robert. ABC random forests for Bayesian parameter inference. *Bioinformatics (Oxford, England)*, 35, 05 2016. doi: 10.1093/bioinformatics/bty867.
- G. J. McLachlan. On bootstrapping the likelihood ratio test statistic for the number of components in a normal mixture. *Journal of the Royal Statistical Society: Series C (Applied Statistics)*, 36(3):318–324, 1987.
- E. Meeds and M. Welling. GPS-ABC: Gaussian process surrogate approximate Bayesian computation. *arXiv preprint arXiv:1401.2838*, 2014.
- N. Meinshausen. Quantile regression forests. *Journal of Machine Learning Research*, 7(35): 983–999, 2006.
- S. A. Murphy and A. Van Der Vaart. On profile likelihood. *Journal of the American Statistical Association*, 95(450):449–465, 2000. doi: 10.1080/01621459.2000.10474219.
- J. Neyman. On the problem of confidence intervals. *Ann. Math. Statist.*, 6(3):111–116, 09 1935. doi: 10.1214/aoms/1177732585.
- J. Neyman. Outline of a theory of statistical estimation based on the classical theory of probability. *Philosophical Transactions of the Royal Society of London. Series A, Mathematical and Physical Sciences*, 236(767):333–380, 1937. ISSN 00804614.
- J. Neyman and E. S. Pearson. On the use and interpretation of certain test criteria for purposes of statistical inference: Part i. *Biometrika*, 20A(1/2):175–240, 1928. ISSN 00063444.
- G. Papamakarios and I. Murray. Fast ϵ -free inference of simulation models with Bayesian conditional density estimation. In D. Lee, M. Sugiyama, U. Luxburg, I. Guyon, and R. Garnett, editors, *Advances in Neural Information Processing Systems*, volume 29, pages 1028–1036. Curran Associates, Inc., 2016.
- G. Papamakarios, D. Sterratt, and I. Murray. Sequential neural likelihood: Fast likelihood-free inference with autoregressive flows. In *The 22nd International Conference on Artificial Intelligence and Statistics*, pages 837–848, 2019.
- G. Papamakarios, E. Nalisnick, D. J. Rezende, S. Mohamed, and B. Lakshminarayanan. Normalizing Flows for Probabilistic Modeling and Inference. *Journal of Machine Learning Research*, 22(57):1–64, 2021.

- G. Peter Lepage. A new algorithm for adaptive multidimensional integration. *Journal of Computational Physics*, 27(2):192 – 203, 1978. ISSN 0021-9991. doi: [https://doi.org/10.1016/0021-9991\(78\)90004-9](https://doi.org/10.1016/0021-9991(78)90004-9).
- U. Picchini, U. Simola, and J. Corander. Adaptive MCMC for synthetic likelihoods and correlated synthetic likelihoods. *arXiv preprint arXiv:2004.04558*, 2020.
- X. Qian, A. Tan, J. Ling, Y. Nakajima, and C. Zhang. The Gaussian CL_s method for searches of new physics. *Nuclear Instruments and Methods in Physics Research Section A: Accelerators, Spectrometers, Detectors and Associated Equipment*, 827(35):63–78, 2016.
- S. T. Radev, U. K. Mertens, A. Voss, L. Ardizzone, and U. Köthe. Bayesflow: Learning complex stochastic models with invertible neural networks. *IEEE Transactions on Neural Networks and Learning Systems*, pages 1–15, 2020. doi: 10.1109/TNNLS.2020.3042395.
- R. Redner. Note on the consistency of the maximum likelihood estimate for nonidentifiable distributions. *The Annals of Statistics*, 9(1):225–228, 1981.
- C. M. Schafer and P. B. Stark. Constructing confidence regions of optimal expected size. *Journal of the American Statistical Association*, 104(487):1080–1089, 2009. doi: 10.1198/jasa.2009.tm07420.
- S. J. Schmidt, A. I. Malz, J. Y. H. Soo, I. A. Almosallam, M. Brescia, S. Cavuoti, J. Cohen-Tanugi, A. J. Connolly, J. DeRose, P. E. Freeman, M. L. Graham, K. G. Iyer, M. J. Jarvis, J. B. Kalmbach, E. Kovacs, A. B. Lee, G. Longo, C. B. Morrison, J. A. Newman, E. Nourbakhsh, E. Nuss, T. Pospisil, H. Tranin, R. H. Wechsler, R. Zhou, R. Izbicki, and T. L. D. E. S. Collaboration). Evaluation of probabilistic photometric redshift estimation approaches for The Rubin Observatory Legacy Survey of Space and Time (LSST). *Monthly Notices of the Royal Astronomical Society*, 499(2):1587–1606, 09 2020. ISSN 0035-8711. doi: 10.1093/mnras/staa2799.
- B. Sen, M. Walker, and M. Woodroffe. On the unified method with nuisance parameters. *Statistica Sinica*, 19(1):301–314, 2009. ISSN 10170405, 19968507.
- S. A. Sisson, Y. Fan, and M. Beaumont. *Handbook of Approximate Bayesian Computation*. Chapman and Hall/CRC, 2018.
- C. J. Stone. Optimal global rates of convergence for nonparametric regression. *The Annals of Statistics*, pages 1040–1053, 1982.
- S. Talts, M. Betancourt, D. Simpson, A. Vehtari, and A. Gelman. Validating Bayesian inference algorithms with simulation-based calibration. *arXiv preprint arXiv:1804.06788*, 2018.
- M. Tanabashi, K. Hagiwara, K. Hikasa, K. Nakamura, Y. Sumino, F. Takahashi, J. Tanaka, et al. Review of particle physics. *Phys. Rev. D*, 98:030001, Aug 2018. doi: 10.1103/PhysRevD.98.030001.
- O. Thomas, R. Dutta, J. Corander, S. Kaski, and M. U. Gutmann. Likelihood-free inference by ratio estimation. *Bayesian Anal.*, 2021. doi: 10.1214/20-BA1238. Advance publication.

- A. B. Tsybakov. *Introduction to Nonparametric Estimation. Revised and Extended from the 2004 French Original. Translated by Vladimir Zaiats*. Springer Series in Statistics. New York: Springer, 2009.
- W. van den Boom, G. Reeves, and D. B. Dunson. Approximating posteriors with high-dimensional nuisance parameters via integrated rotated Gaussian approximation. *Biometrika*, Aug 2020. ISSN 1464-3510. doi: 10.1093/biomet/asaa068.
- P. Virtanen, R. Gommers, T. E. Oliphant, M. Haberland, T. Reddy, D. Cournapeau, E. Burovski, P. Peterson, W. Weckesser, J. Bright, S. J. van der Walt, M. Brett, J. Wilson, K. J. Millman, N. Mayorov, A. R. J. Nelson, E. Jones, R. Kern, E. Larson, C. J. Carey, Í. Polat, Y. Feng, E. W. Moore, J. VanderPlas, D. Laxalde, J. Perktold, R. Cimrman, I. Henriksen, E. A. Quintero, C. R. Harris, A. M. Archibald, A. H. Ribeiro, F. Pedregosa, P. van Mulbregt, and SciPy 1.0 Contributors. SciPy 1.0: Fundamental Algorithms for Scientific Computing in Python. *Nature Methods*, 17:261–272, 2020. doi: 10.1038/s41592-019-0686-2.
- A. Wald. Tests of statistical hypotheses concerning several parameters when the number of observations is large. *Transactions of the American Mathematical society*, 54(3):426–482, 1943.
- L. Wasserman, A. Ramdas, and S. Balakrishnan. Universal inference. *Proceedings of the National Academy of Sciences*, 117(29):16880–16890, 2020.
- S. Weinzierl. Introduction to Monte Carlo methods. *arXiv preprint arXiv:hep-ph/0006269*, 2000.
- R. Wilkinson. Accelerating ABC methods using Gaussian processes. In *Artificial Intelligence and Statistics*, pages 1015–1023, 2014.
- S. S. Wilks. The large-sample distribution of the likelihood ratio for testing composite hypotheses. *Ann. Math. Statist.*, 9(1):60–62, 03 1938. doi: 10.1214/aoms/1177732360.
- S. Wood. Statistical inference for noisy nonlinear ecological dynamic systems. *Nature*, 466:1102–4, 08 2010. doi: 10.1038/nature09319.
- Y. Yang, A. Bhattacharya, and D. Pati. Frequentist coverage and sup-norm convergence rate in Gaussian process regression. *arXiv preprint arXiv:1708.04753*, 2017.
- Y. Zhu, X. Shen, and W. Pan. On high-dimensional constrained maximum likelihood inference. *Journal of the American Statistical Association*, 115(529):217–230, 2020.